

Understanding aqueous foam with novel CO₂-soluble surfactants for controlling CO₂ vertical sweep in sandstone reservoirs

Guangwei Ren^{1,2} · Quoc P. Nguyen¹

Received: 30 July 2016 / Published online: 28 March 2017
© The Author(s) 2017. This article is an open access publication

Abstract The ability of a novel nonionic CO₂-soluble surfactant to propagate foam in porous media was compared with that of a conventional anionic surfactant (aqueous soluble only) through core floods with Berea sandstone cores. Both simultaneous and alternating injections have been tested. The novel foam outperforms the conventional one with respect to faster foam propagation and higher desaturation rate. Furthermore, the novel injection strategy, CO₂ continuous injection with dissolved CO₂-soluble surfactant, has been tested in the laboratory. Strong foam presented without delay. It is the first time the measured surfactant properties have been used to model foam transport on a field scale to extend our findings with the presence of gravity segregation. Different injection strategies have been tested under both constant rate and pressure constraints. It was showed that novel foam outperforms the conventional one in every scenario with much higher sweep efficiency and injectivity as well as more even pressure redistribution. Also, for this novel foam, it is not necessary that constant pressure injection is better, which has been concluded in previous literature for conventional foam. Furthermore, the novel injection strategy, CO₂ continuous injection with dissolved CO₂-soluble surfactant, gave the best performance, which could lower the injection and water treatment cost.

Keywords Foam · CO₂-soluble surfactant · Sweep efficiency · Gravity segregation · Optimal injection strategy

1 Introduction

Gases have been used as driving fluids in improved oil recovery processes since 1900 (Lake 1989), in which CO₂ flooding has attracted a lot of attention because of its proven miscible-like displacement (Stalkup 1983), high availability, and environmental concerns. However, this process frequently experiences viscous fingering, gravity override, and gas channeling because of reservoir heterogeneity as well as low density and viscosity of CO₂, which results in a decreased oil recovery (Rossen and Renkema 2007). Fortunately, the use of foam can reduce gas mobility and effects of heterogeneity and therefore increase sweep efficiency (Rossen 1995). This was first proposed in 1958 by Bond and Holbrook (1958). Carbon dioxide (CO₂) foams in porous media with aqueous soluble surfactants have been widely studied in connection with their application in enhanced oil recovery (EOR) (Lee and Heller 1988; Du et al. 2007). These experimental and theoretical studies have contributed to the success of several field foam applications (Patzek 1996), especially for carbonate reservoirs (Hoefner et al. 1995; Stevens 1995). Unfortunately, field experiences have shown that conventional foams with only aqueous soluble surfactants have some important limitations. For example, the injected surfactant slugs do not improve the CO₂-oil contact. Gravity override and macroscopic heterogeneity also challenge the success of surfactant placement into thief zones where the presence of foam is desired.

Gravity segregation leads to poor sweep efficiency and has received great attention because of its importance in

✉ Guangwei Ren
guangweiren@utexas.edu

¹ Petroleum and Geosystems Engineering Department,
University of Texas at Austin, Austin, TX, USA

² Present Address: Total E&P R&T USA, Houston, TX, USA

EOR processes involving gas injection. An analytical model developed by Stone (1982) for gravity segregation of water and gas provided a conceptual framework for understanding gravity segregation without foam. He assumed that gas was incompressible and there were negligible gradients of capillary pressure. After a steady state was established, there were three zones in the reservoir (Fig. 1): a gas zone at the top with gas, a water zone at the bottom with only water, and a mixed zone with both gas and water flowing. Jenkins (1984) extended this study and provided a solution to determine the saturation profile and shapes of three zones. Rossen and van Duijn (2004) showed that the theoretical justifications presented by Stone and Jenkins for their models were incorrect, but they can be derived rigorously with only some assumptions (Rossen et al. 2006; Rossen and Shen 2007; Jamshidnezhad et al. 2008a).

Stone’s model may be applied to foam processes that obey the “fixed limiting capillary pressure” (Rossen et al. 1994, 1995b). Therefore, Shi and Rossen (1996) proposed that for foam in a cylindrical reservoir:

$$\left(\frac{R_g}{R_e}\right)^2 = VGR = \frac{1}{N_g} \frac{1}{R_L} = \left(\frac{\nabla P^f(R_g)}{\Delta\rho g}\right) \left(\frac{2R_g H k_x}{R_e^2 k_z}\right) \quad (1)$$

where R_e is the reservoir radius; R_g is the radial position at which gas and water flows are completely segregated; N_g is the gravity number, the ratio of the vertical driving force for segregation to the horizontal pressure gradient; VGR represents the viscous-to-gravity ratio; R_L is a modified reservoir aspect ratio; N_g and R_L are evaluated at the radial position R_g at which gas and water flows are completely segregated; $\Delta\rho$ is the density difference between gas and liquid; $\nabla P^f(R_g)$ is the pressure gradient in the foam bank near the injection well in the absence of gravity segregation and is a simple function of water flow rate and water saturation (Friedmann et al. 1991); H is the reservoir height; k_z and k_x are the vertical and horizontal absolute permeabilities; and g is the gravity acceleration constant. This result implied that for a given reservoir with density differences between phases, the only way to increase the distance that gas and water travel together before complete segregation was to increase the horizontal pressure gradient

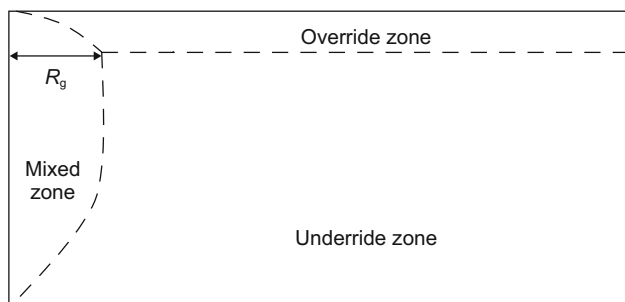


Fig. 1 Three zones during gas injection

(Rossen and Shen 2007). Because of nonuniform mobility in the foam bank for surfactant solution alternating gas (SAG) and the differences between processes, the criteria for gravity override with co-injection (Shi and Rossen 1996) cannot be simply applied to SAG (Shi et al. 1998).

In addition to water flooding, pure gas flooding, water alternating gas (WAG) (Ma and Youngren 1994), and simultaneous WAG (SWAG) (Sanchez 1999), heretofore, some additional injection strategies in the presence of foam can be classified as:

- (1) *Co-injection: simultaneous injection of surfactant solution with gas*

Most of the laboratory experiments were conducted in this manner (Svorstol et al. 1996; Mohd Shafian et al. 2015), even though it was tried in only few fields (Blaker et al. 1999) since it may lead to fractures due to high back pressure. Chen et al. (2012) and Elhag et al. (2014) demonstrated that apparent viscosities of foams measured with a capillary viscometer were more than 8 cP at variable temperatures and foam qualities with a switchable ethoxylated cationic CO₂-philic surfactant. They found that the delivery media of CO₂-soluble surfactant imposed less impact. Later, further tests on a 1.2 Darcy glass bead pack and a 49-mD dolomite core gave apparent viscosities of foams as high as 390 and 100 cP, respectively (Chen et al. 2015). Xing et al. (2012) and McLendon et al. (2014) measured the pressure drop across a Berea sandstone core as the CO₂/surfactant solution was injected with selected branched ethoxylated CO₂-soluble surfactants, which gave a weak foam with a mobility reduction factor around five. Through simulation with an analytical model, Rossen et al. (2006) drew a series of conclusions concerning the optimal injection strategy for co-injection with conventional water-soluble surfactants, regarding longer gravity segregation length. Recently, Zeng et al. (2016) demonstrated a spreading effect caused by different partition coefficients of CO₂-soluble surfactants based on published data (Ren et al. 2013) through 1D simulation during co-injection. Surfactants were injected with brine even though they are CO₂-soluble.

- (2) *SAG or foam-assisted WAG (FAWAG)*

For SAG, surfactant is added to a water cycle and the actual diverting foam is generated in a subsequent gas cycle. Some experiments on laboratory scale have been conducted (Lawson and Reisberg 1980; Xu and Rossen 2003). It was shown that a higher injection rate will promote stronger foam generation (Mohd Shafian et al. 2015). Rossen et al. (1995a) pointed out SAG foam processes can combine high gas injectivity with low mobility at the front of the foam bank, which offers an escape from the dilemma posed by early modeling, i.e., improved vertical sweep of

gas with foam requires an increase in injection pressure (Shi et al. 1998). Shan and Rossen (2004) proposed an optimal injection strategy for overcoming gravity override with foam in a homogeneous reservoir. Kloet et al. (2009) extended the study of Rossen and Renkema (2007) and developed design criteria for the optimal foam strength and slug size for a given permeability contrast between layers. SAG injection also minimizes contact between water and gas in surface facilities and piping (Heller 1994). Relative to co-injection, SAG could overcome gravity override better and improve injectivity (Patzek 1996; Shi and Rossen 1996; Blaker et al. 1999). Sagir et al. (2014c, d) conducted pure CO₂ injection after surfactant solution flooding to mimic FAWAG with a new CO₂-soluble surfactant using Berea cores, during which a mobility reduction factor of 3.1 was achieved. Similar results were demonstrated by Xing et al. (2012) and McLendon et al. (2014) relative to pure CO₂ injection on carbonate and sandstone cores. Recently, 80 cP of foam apparent viscosity was achieved by Chen et al. (2015) in a 49-mD dolomite core with a switchable ethoxylated cationic CO₂-philic surfactant.

(3) WAG with dissolved surfactant (WAGS)

Relative to the conventional SAG, WAGS delivers the surfactant in the CO₂ phase, which may increase the CO₂-oil contact. Le et al. (2008) conducted both SAG and WAGS at the same conditions, which resulted in similar ultimate oil recoveries and pressure drops.

(4) Novel CO₂ injection: CO₂ continuous injection with dissolved CO₂-soluble surfactant

CO₂ continuous injection with dissolved CO₂-soluble surfactant is another novel concept, which is the extreme case of WAGS and may not require brine injection. Foam is created in situ as CO₂ and dissolved surfactant propagate through the formation mixing with reservoir brine to maximize the benefit of CO₂-miscible displacement and improve the injectivity. Similar to WAGS, this method improves in situ foam generation, drastically lowers the injection costs, and reduces the loss of surfactant onto the rock surface due to adsorption. Xing et al. (2012) and McLendon et al. (2014) showed that the mobility reduction factor was around two, which was slightly higher than pure CO₂ injection on pre-saturated cores. In Le et al. (2008), experimental and field scale simulation results show this is the most promising injection scenario which gave highest oil recovery and injectivity. Field trials indicated a 30% sweep efficiency improvement (Sanders et al. 2012).

Supercritical carbon dioxide (scCO₂) with its easily attainable critical temperature and pressure (31.1 °C and 7.38 MPa) can be viewed as an ideal chemical processing solvent because it is nontoxic, inexpensive, volatile,

nonflammable, readily available in large quantities, and environmentally benign (Eastoe et al. 2001). However, because of its very low dielectric constant with weak intermolecular forces and low polarizability per volume and correspondingly weak van der Waals forces (O'Shea et al. 1991), CO₂ is a poor solvent for high molecular weight, hydrophilic molecules, and polar compounds. In the past decades, several approaches have been explored to enhance the solubility of polar substances in scCO₂ (Hoeffling et al. 1993; McHugh and Krukonić 1994). Eastoe et al. (2003) reported stability and aggregation structures of various economically viable surfactants for CO₂. Results confirmed the affinity of methyl-branched tails for CO₂ but still contributing limited solubility. A review article from Eastoe et al. (2006) told the story of small-molecule CO₂-active surfactants, from fluorinated compounds to oxygenated amphiphiles. Xing et al. (2012) screened solubility of several commercially available nonionic surfactants in CO₂, and the most stable foams were obtained with branched alkylphenol ethoxylates which exhibited 0.01wt%–0.1wt% solubility in CO₂. A lot of effort has put into obtaining low toxicity and low price CO₂-soluble surfactants, of which non-fluorinated AOT (sodium bis(2-ethylhexyl)-sulfosuccinate) (Eastoe et al. 2001; Liu and Erkey 2001) and nonionic surfactants (Liu et al. 2001; Xing et al. 2012) were of most interest. Dhanuka et al. (2006) noted that DOW Tergitol TMN 6 was an effective foaming agent characterized by stable, white, and opaque foams formed at 25 °C and 345 bar. Fan et al. (2005) established that oligo vinyl acetate (OVAc) is extremely CO₂-philic and suitable for incorporation into CO₂-soluble ionic surfactants. Tan and Cooper (2005) used polyethylene oxide (PEO) as the hydrophile during their design of tri-block OVAc-b-PEO-b-OVAc surfactants capable of stabilizing CO₂ foam. Sanders et al. (2010) reported the design and synthesis of a new class of twin-tailed surfactants based on glycerin and designed for the scCO₂-water interface, whose performance was better than a linear secondary alcohol CO₂-soluble surfactant. Adkins et al. (2010a, b) and Chen et al. (2010) have proven that a branched hydrocarbon nonionic surfactant can effectively reduce the contact of CO₂ and water phases and raise the surface pressure and the surfactant efficiency (the concentration to produce 20 mN/m interfacial tension reductions). Chen et al. (2012) developed a switchable ethoxylated cationic CO₂-philic surfactant which was able to stabilize CO₂/water foams up to 182 g/L at 120 °C, 3400 psia. Those hybrid surfactants combined the high cloud points of ionic surfactants with high solubility in CO₂ of nonionic surfactants. The adsorption characteristics of this surfactant were described by Cui et al. (2014), and the interfacial tension (IFT) between CO₂/water was around 5 mN/m (Elhag et al. 2014). Sagir et al. (2014a, b) synthesized several CO₂-philic surfactants using maleic anhydride with either 4-tert-butylbenzyl

alcohol or dipropylene tertiary butyl alcohol. The IFT between CO₂/brine could reach 1.93 to 4.2 mN/m. The surfactant used here was a new branched nonionic hydrocarbon surfactant with suitable combination of PPO (poly(propylene oxide)) and PEO (poly(ethylene oxide)).

The notion of applying a CO₂-soluble surfactant during an EOR process to generate C/W mobility control foams was suggested by Bernard and Holm (1967). Soong et al. (2009) probed two strategies for using CO₂-soluble compounds to decrease the mobility of scCO₂, “direct thickening” of CO₂ which is accomplished by a macroemulsion formed by an associated thickener in scCO₂, and in situ foam generation. Several laboratory experiments with distinct CO₂-soluble surfactants have been conducted with variable injection strategies, which will be reviewed below. Either liquid or CO₂ phase could be used to delivery those novel surfactants. A field trial was carried out in west Texas using surfactant injection in the CO₂ phase to create a CO₂-in-water emulsion or foam to improve vertical conformance and create in-depth mobility control (Sanders et al. 2012). Results indicated a 30% CO₂ trapping improvement in situ.

In a previous publication (Le et al. 2008), a novel foam concept was proposed and a surfactant concentration of 0.1wt% in CO₂ at ambient temperature and 1800 psi was roughly determined. Oil recoveries with variable injection strategies were presented briefly. In our earlier work (Ren et al. 2014), solubility and partition coefficients of a series of nonionic CO₂-soluble surfactants have been tested at varying pressures, temperatures, and salinity in our laboratory. Preliminary probes have revealed superiorities of CO₂-soluble surfactant foam over conventional aqueous soluble surfactant foam through laboratory core floodings of Silurian dolomite carbonate and field scale simulations (Ren et al. 2013). However, the conclusions drawn previously deserve to be further examined with broader rock types and injection strategies. Moreover, some conclusions from prior literature based on conventional surfactants, such as optimal injection strategy, could be updated or modified in the presence of CO₂-soluble surfactants. Through laboratory experiments and field scale simulations, in the current paper, we will peruse the following goals: demonstrate the remarkable advantages of CO₂-soluble surfactant on the laboratory scale with co-injection, alternating injection, and novel pure CO₂ injection with dissolved surfactant; with field scale simulation, exhibit the considerable superiorities of CO₂-soluble surfactant over conventional aqueous surfactant through SAG and co-injection with variable perforation interval or slug size; investigate the unique characteristics of the novel CO₂ foam, including surfactant delivery media, optimal injection strategy, and some additional considerations; and then, examine whether previous conclusions in the literature for

conventional surfactants were still valid for this novel foam with our practical postulations.

2 Experimental section

2.1 Materials

A 2-ethylhexanol (2-EH) alkoxyate nonionic hydrocarbon surfactant, which has been used in a previous study (Ren et al. 2013) and named S, and a commercially available anionic surfactant (CD 1045) which is not soluble in CO₂, were used in this study. The properties of S at variable pressures, temperatures, and salinity, such as solubility in CO₂, partition coefficient between brine and CO₂, and aqueous stability have been studied in earlier work (Ren et al. 2014). The adsorptions of the used surfactants are neglected due to negative surface charges of sandstone samples at neutral pH (Lawson 1978; Mannhardt et al. 1993) and without the presence of clay in used outcrop. Except for novel CO₂ continuous injection with dissolved CO₂-soluble surfactant, in all other core flood experiments, the surfactant solution containing 0.2wt% surfactant and 3wt% NaCl (analytical grade quality) was used to stabilize supercritical CO₂ foam generated in 1-ft-long Berea sandstone cores. The same NaCl concentration was used to saturate the core with brine before injection of the surfactant solution and CO₂. The purity of the liquid CO₂ was 99.5%. The rock permeability to brine was around 300 mD.

2.2 Experimental apparatus and procedures

A schematic of the core flood setup is shown in Fig. 2. It is comprised of three main modules: a fluid injection system, core holder and pressure transducers, and a back pressure and effluent collection system.

Fluid injection system A TELEDYNE ISCO Model 500D syringe was used to directly inject brine or surfactant solution into the cores. CO₂ was displaced into the core by deionized (DI) water through a high pressure accumulator that had a piston to separate water from CO₂.

Core holder and pressure transducers A Phoenix Hassler-type core holder with capacity for 2-inch-diameter core was mounted vertically, and fluids were injected from the top to the bottom. Hydraulic oil was used as an overburden fluid, which compressed and sealed the 0.25-inch-thick rubber sleeve to assure the axial flow of the injection fluids, and to prevent leakage. There were five pressure taps along the side of the core holder in the vertical direction, which connected two absolute pressure transducers (Channel 1 and 5) and three differential transducers (Channel 2, 3 and 4). The differential transducers detected

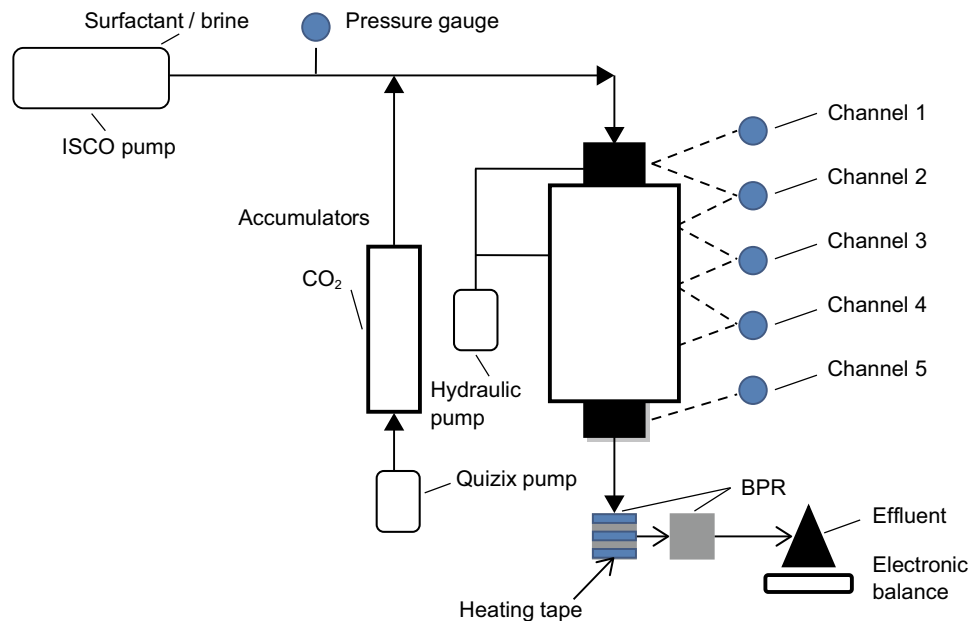


Fig. 2 Schematic of an experimental setup for core flooding

the pressure drops over sections along the core from the top, whose lengths were 2, 4, and 4 inches and denoted as Sect. 1, 2, and 3, respectively.

Back pressure regulator (BPR) and effluent collector Two BPRs were used in series to maintain a constant back pressure of 1500 psig during core flooding. The first BPR placed immediately at the outlet of the core holder was set at 1500 psig, and the second BPR set at 1100 psig.

Core preparation The core was cleaned and dried in a convection oven at 110 °C for 48 h. It was then wrapped in three layers of aluminum foil and a thin Teflon heat shrink tube to prevent CO₂ diffusion and penetration. The wrapped core was placed in the core holder and evacuated for 10 h before the core was saturated with brine (3wt% NaCl) for porosity measurement. The permeability of the brine-saturated core was determined from Darcy's law.

Foam flooding All core floods were conducted at 35 °C and 1500 psi back pressure. Three injection strategies were examined without using the pre-generator. These were simultaneous injection of CO₂ and surfactant solution, alternating injection, and CO₂ continuous injection with dissolved CO₂-soluble surfactant. Except for the last one, surfactants were always injected with brine even though the novel surfactant is CO₂-soluble. It will partition into CO₂ instantaneously when two phases contact. The impact of delivery media on the novel foam performance is out of the scope of this study and will be discussed in a separate publication. To obtain a fixed injection foam quality of 75% for co-injection, the injection rates of the surfactant solution (containing 0.2 wt% surfactant) and CO₂ were fixed at 0.1 cc/min and 0.3 cc/min, respectively. Through

adjusting injection time individually, slug sizes of the surfactant solution and gas in alternating injection were kept at 0.1 PV and 0.2 PV, respectively. For the third novel strategy, 0.6 cc/min was employed for CO₂ injection. The surfactant needed in CO₂ in the container was determined by the known container volume, CO₂ density (0.494 g/cc under experimental conditions), and fluid injection rates, to maintain the mass injection rate the same as in other scenarios. After calculation, 0.1wt% in CO₂ was used to maintain the same amount of surfactant per minute to be injected in different strategies. Pressure drops over the three sections of the core were recorded. Water saturation was determined based on the difference in cumulative mass between the injected and the produced waters.

3 Simulation description

3.1 Reservoir model

A 15° sector of a cylindrical homogenous reservoir, 100 ft thick and 440 ft in radius, was used for all simulations in this work. Porosity is 20%. The vertical and horizontal permeabilities are 400 and 200 mD, respectively. The reservoir model was numerically constructed using 100 grid blocks in the radial direction and 20 grid blocks in the vertical direction. A vertical injector is placed at the center of the reservoir and fully completed over 100 ft along, while a parallel fully penetrating producer is placed in the outer boundary grids whose permeability is set to 10,000 Darcy to simulate an open boundary reservoir and prevent

artificial gas back flow (Namdar Zanganeh and Rossen 2013). The radial grid size increases from 3 ft for the first 30 grids from the injector to 5 ft for the remaining grid blocks. Leeftink et al. (2013) found that a fine grid resolution near the injection well is important to prevent underestimating the effects of dry-out increasing injectivity in a SAG process in finite-difference simulations. The schematic is shown in Fig. 3. The reservoir is isothermal at 35 °C, and the initial reservoir pressure is 1500 psi. For the sake of simplification, only the water phase is present in the reservoir initially (Kloet et al. 2009) since foam is only beneficial to sweep efficiency. All simulations were conducted with the Computer Modeling Group’s STARS simulator.

The heuristic foam model built in CMG/STARS has been introduced in the literature (Zeng et al. 2016) and widely used in foam process simulation (Farajzadeh et al. 2015). Model parameter values fitting through different algorithms have been discussed by several researchers (Ma et al. 2014; Rossen and Boeije 2015). In our current work, the surfactant concentration and dry-out effects are considered and some typical values are chosen, as shown in Table 1. Here, we chose 100 for *fmmob*, which is less than these employed by earlier researchers, such as 1000 (Rossen et al. 2006), 3000 (Rossen and Shen 2007; Jamshidnezhad et al. 2008a), or 5000 (Cheng et al. 2000; Rossen and Renkema 2007; Kloet et al. 2009), because we believe too strong foam used previously masked some details in the foam process, which is crucial for the novel foam. Meanwhile, it is also much less than the result of coreflood matching (Ma et al. 2013) because the foam in 3D is much weaker than in 1D, which has been demonstrated by Li et al. (2006). In simulations, we made *fmsurf* equal to the injected surfactant concentration (3.34×10^{-5} , molar fraction) (Hanssen et al. 1994; Rossen and Renkema 2007). A linear dependence between foam strength and surfactant concentration was chosen (*epsurf* = 1) (Rossen and Renkema 2007). Here, we set the

Table 1 Foam model parameters used in field scale foam process simulation

Parameter	<i>fmmob</i>	<i>fmsurf</i>	<i>epsurf</i>	<i>fmdry</i>	<i>epdry</i>
Value	100	3.34×10^{-5}	1	0.15	1

epdry regulates the slope of *kr_g* curve near *fmdry*
epsurf regulates foam strength for surfactant concentration below *fmsurf*
fmdry critical water saturation at which foam experiences significant coalescence
fmmob reference mobility reduction factor
fmsurf surfactant concentration for full-strength foam

fmdry as 0.15, which is more than irreducible water saturation. The reasons that we do not attempt to derive those parameters from laboratory scale history matching are threefold. The first, heretofore, the empirical model used in STARS is based on pseudo-steady-state assumption that the local equilibrium is achieved instantaneously without accounting for transient behavior of foam (Fisher et al. 1990; Rossen and Renkema 2007; Jamshidnezhad et al. 2008a). Therefore, it is suspected that the model may be more suitable for field scale simulation but not for laboratory scale. The second, there is no consensus on how to scale up foam behavior and corresponding parameters from laboratory to field. Hence, typical values are chosen. The third, it is of most importance to examine the relevant foam behavior discrepancy between different injection strategies and surfactants, rather than absolute performances, as long as the same parameter values are used.

3.2 Injection scheme

Injection schemes were composed of two modules, in which constant rate mode is examined followed by

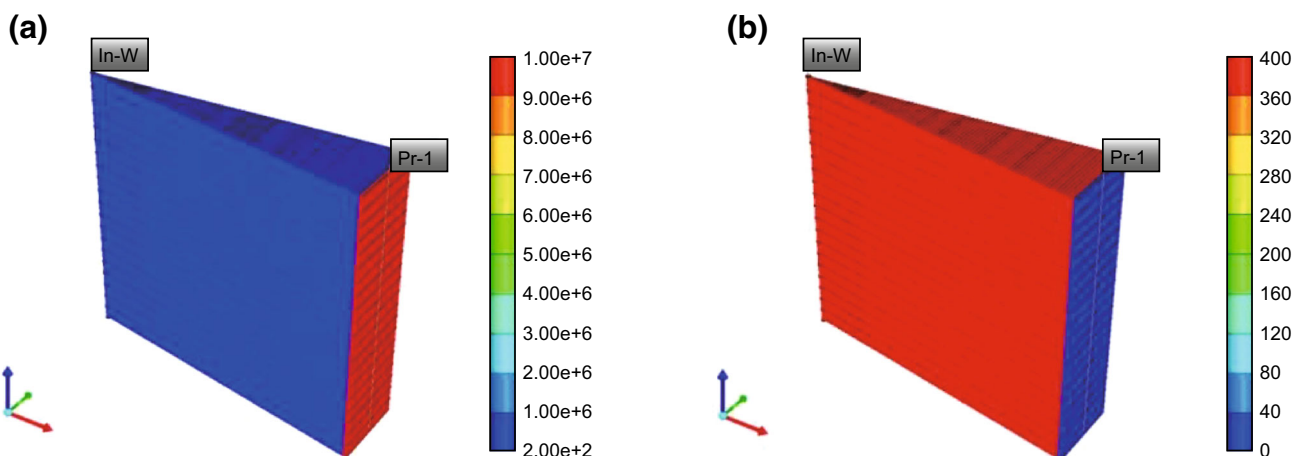


Fig. 3 Cylindrical reservoir model employed in field scale simulations. **a** Permeability I and J directions. **b** Permeability K direction

constant pressure mode. In each mode, SAG, co-injection, and CO₂ continuous injection with dissolved CO₂-soluble surfactant are presented, as summarized in Table 2. Relative to a previous publication (Le et al. 2008), it is the first time that the measured surfactant partition coefficients of CO₂-soluble surfactant between two phases (Ren et al. 2014) have been used in field scale simulations.

The first strategy is the alternating injection of the surfactant solution and gas (surfactant alternating gas, SAG), in which the novel surfactant is injected with brine even though it is CO₂-soluble. The liquid/gas slug size ratio is kept at 1:1 in volume. Two different slug sizes are tested, 36.5 and 182.5 days, respectively.

Then, co-injection is examined, either two phases in the same intervals (simultaneous injection through all perforation, SIAP, or simultaneous injection through partial perforation, SIPP), or water into the upper part while gas into the lower part (separate injection no barrier, SINB, or separate injection with barrier, SIWB). Stone (2004a, b) proposed injection of water in an interval above the gas to increase reservoir sweep, which is called “modified SWAG” by Algharaib et al. (2007). The main goal of separate injection is to reduce the effect of gravity segregation commonly encountered in gas–liquid flow in reservoirs with high vertical communication (Rossen et al. 2006; Liu et al. 2011).

A schematic of the four strategies is shown in Fig. 4. For constant pressure mode, only the best case selected from the constant rate mode, SINB, is displayed.

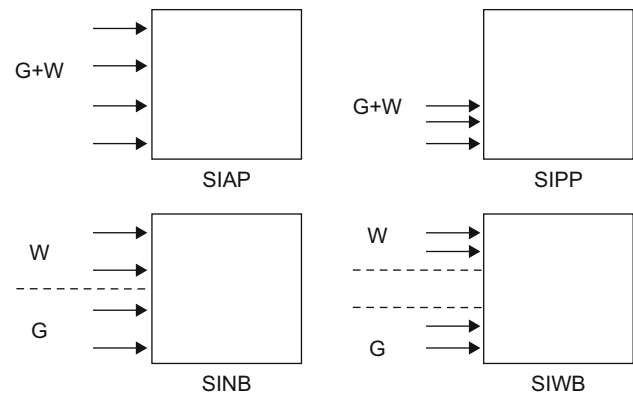


Fig. 4 Four different injection strategies for simultaneous injection of the surfactant solution and CO₂ (*G* gas, *W* water)

At last, the novel strategy, CO₂ continuous injection with dissolved CO₂-soluble surfactant, was conducted for both modes with variable perforations. This is a unique one in which the surfactant concentration in CO₂ after splitting between phases during injection should be lower than its maximum solubility (Ren et al. 2014).

Table 2 summarizes the design parameters for the injection strategies described above. CO₂ and water injection rates are chosen so as to achieve approximately 75% foam quality under reservoir conditions. Doubled injection time is employed to inject the same amount of fluids. The selection of injection pressure at the constant pressure injection mode is discussed in details in the corresponding section.

Table 2 Simulation scenarios for variable injection modes and strategies

Injection strategies			Water/ CO ₂ cycle ratio	Water cycle, day	Water rate, bbl/d	CO ₂ rate, scf/d	Water injection pressure, psi	CO ₂ injection pressure, psi	Injection surfactant concentration, molar fraction	Total injected, PV/ Years
Constant rate mode	Alternating injection	SAG	1:1	36.5 and 182.5	45	90,000	–	–	3.34×10^{-5}	5.76/16
		Co-injection	SIAP	–	–	45	90,000	–	–	3.34×10^{-5}
		SIPP	–	–	45	90,000	–	–	3.34×10^{-5}	5.76/8
		SINB	–	–	45	90,000	–	–	3.34×10^{-5}	5.76/8
		SIWB	–	–	45	90,000	–	–	3.34×10^{-5}	5.76/8
	Novel CO ₂ injection	All perforation	–	–	–	115,714.3	–	–	9.54×10^{-5}	5.76/8
	Partial perforation	–	–	–	115,714.3	–	–	9.54×10^{-5}	5.76/8	
Constant pressure mode	Alternating injection	SAG	1:1	36.5 and 182.5	–	–	1547	1581	3.34×10^{-5}	5.76/16
		Co-injection	SINB	–	–	–	1598	1608	3.34×10^{-5}	5.76/8
	Novel CO ₂ injection	All perforation	–	–	–	–	1585	–	9.54×10^{-5}	5.76/8

We employ the CO₂ storage, R_g (gravity segregation length), and CO₂ utilization ratio as evaluation criteria. The CO₂ storage is defined as CO₂ staying in the reservoir at the end of injection under surface conditions, which directly reflects the sweep efficiency. CO₂ utilization ratio is defined as the ratio of CO₂ storage over cumulative CO₂ injection, which would be more useful to reflect the economic concern.

4 Results and discussion

4.1 Experimental results

4.1.1 Co-injection

The sectional pressure drops of two types of foams are shown in Fig. 5. For the conventional foam, a strong foam started to propagate into Sect. 2 at 8 IPV (total injected pore volume) and then Sect. 3 as late as 15 IPV. On the contrary, the novel foam displayed higher foam strength and earlier pressure response in each section, at 5 IPV and 12 IPV, respectively. However, this is more attributed to the superior and essential ability of the novel surfactant to stabilize the bubble film than improved foam propagation (Ren et al. 2013) or surfactant spreading effect (Zeng et al. 2016) since foam will not directly affect the liquid propagation and the surfactant already spreads to the whole core with current injection quality. In prior publications, it was found that intermediate partition ability of the novel surfactant could significantly improve foam propagation owing to higher mobility of the gas phase than the aqueous phase. However, too high a partition coefficient may adversely impact foam propagation due to the local surfactant concentration being lower than the critical value, which is the so-called spreading effect. Nevertheless, this

effect may play a less important role compared with surfactant stabilization capacity on bubbles since more than 1 PV liquid has been injected when a significant pressure drop is observed. Adkins et al. (2010b) reported that the CO₂-philic nonionic surfactant used here could lower the gas/water interfacial tension to 5.6 mN/m (2000 psia @ 24 °C, 0.01wt%). This remarkably outruns highly commercialized surfactant CD-1045 that has an interfacial tension of 9.5 mN/m under similar conditions (Grigg 2004). Specifically, with approximate calculation, the apparent viscosity exhibited by the tested novel surfactant was either comparable (Chen et al. 2015) or at least two magnitudes higher than other CO₂-soluble surfactants (Sanders et al. 2010; Xing et al. 2012; McLendon et al. 2014). Outstanding stability of a bubble film contributes the earlier pressure drop response and stronger foam, which is also revealed by water saturation curves, shown in Fig. 6. For the novel foam, preceding the strong foam presence, the weak foam begin to displace water immediately after gas breakthrough and, then, gradually toward the residual water saturation (0.2). On the contrary, for the conventional foam, a lack of high pressure drop causes the displacement curve to level off earlier and the residual water saturation is much higher (0.46). Relative to carbonate, sandstone tends to give more uniform pore size distribution and smaller pores, which contributes to higher water saturation at gas breakthrough and residual values.

4.1.2 Alternating injection

Figure 7 demonstrates the sectional pressure drop performances for conventional and novel foams. For both types of foams, we observed that the pressure drops built up during liquid injection and declined in the following gas injection, then they tended to fluctuate from cycle to cycle (Lawson and Reisberg 1980). As we observed above for

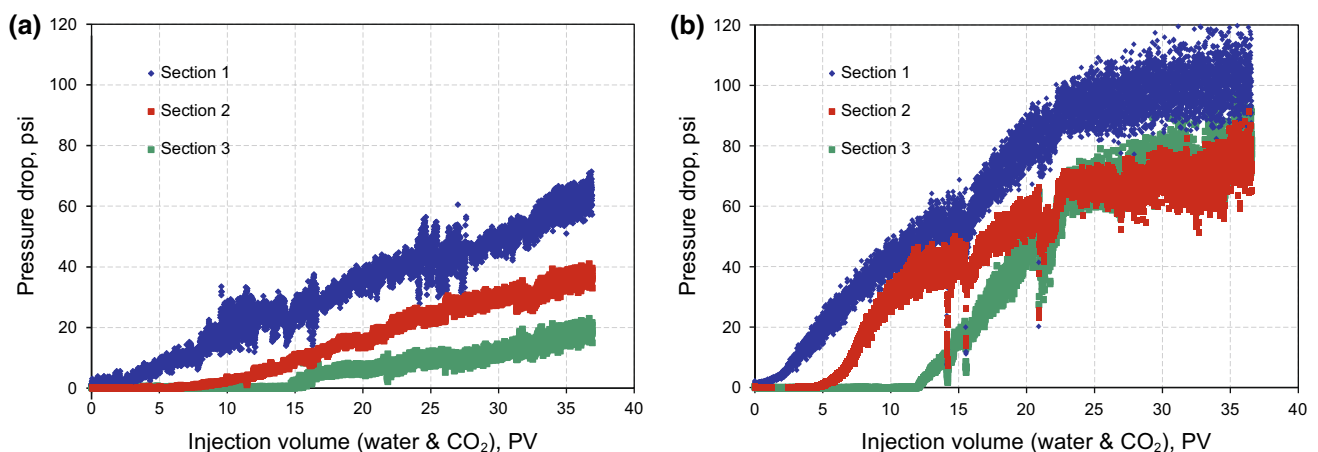


Fig. 5 Pressure drops across the core during simultaneous injection. **a** Conventional foam. **b** Novel foam

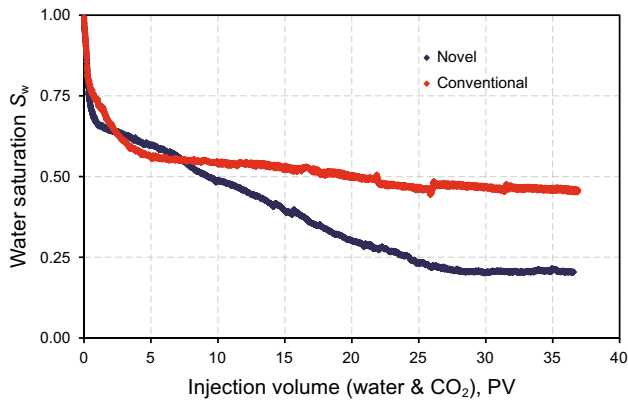


Fig. 6 Average water saturation in the core during simultaneous injection

co-injection, here the contrast became more significant both in pressure drop magnitude and in strong foam propagation. For the novel foam, it only took 1 IPV into Sect. 2 and then 5 IPV to reach Sect. 3. On the contrary, double the amount of fluids were required for the conventional foam to obtain some response. It is well known that the sandstone holds a negative surface charge under the normal formation pH (6–7.5). In turn, the anionic (CD 1045) and nonionic (novel surfactant) surfactants should be close to the adsorption level without the presence of a large amount of clay. Therefore, the novel CO_2 -soluble surfactant really improves the strong foam propagation without any concern about surfactant adsorption. Meanwhile, the magnitude of the pressure drop for the novel foam is 5 to 10 times higher than that of the conventional foam, which also proves the superior ability of the CO_2 -soluble surfactant to stabilize the bubble film over only aqueous soluble surfactant. Furthermore, the apparent viscosity of the novel foam achieved here is either comparable to (Chen et al. 2015) or almost two magnitudes higher than those in

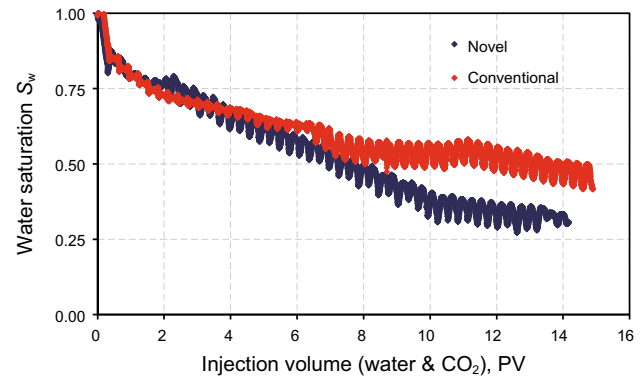


Fig. 8 Average water saturation in the core during alternating injection

the literature with other CO_2 -soluble surfactants (Xing et al. 2012; McLendon et al. 2014; Sagir et al. (2014c, d).

Correspondingly, the residual water saturation after foam propagation has been lowered from 0.42 (conventional) to 0.31 (novel), as shown in Fig. 8, and the displacement efficiency has been improved almost 20%. At the same time, we also notice that relative to simultaneous injection (Fig. 6), the alternating injection does promote the foam generation and injectivity (Li and Rossen 2005) for both types of foams indicated by the quick strong foam propagation and lower pressure drops.

4.1.3 CO_2 continuous injection with dissolved CO_2 -soluble surfactant

The pressure drops and water saturation in the displacement process are shown in Fig. 9. As mentioned in the prior section, the same amount of surfactant per time was injected in the co-injection and the current novel strategy, which eliminated possible bias during comparison. Propagation of the strong foam was accordingly observed in

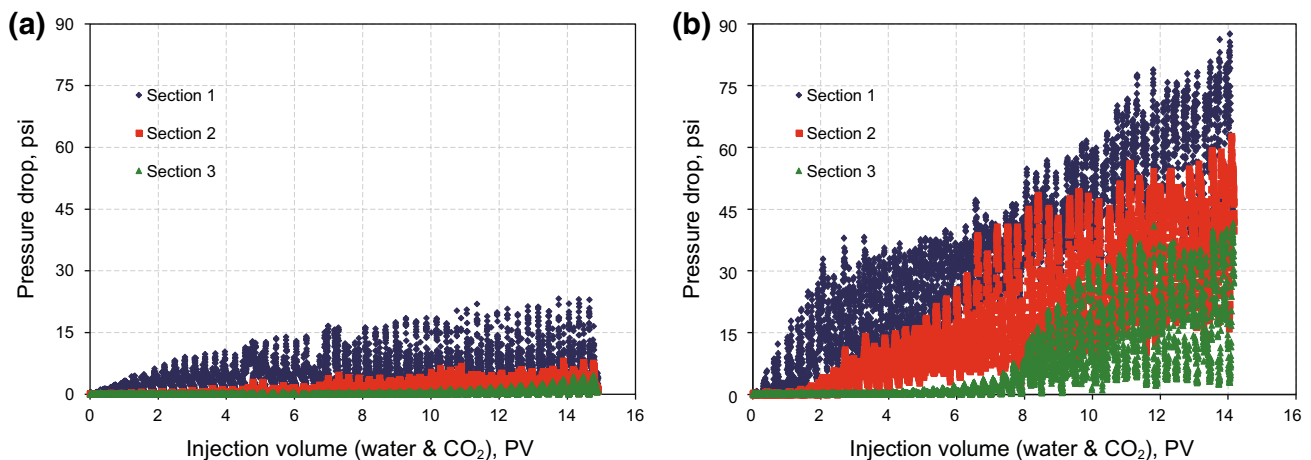


Fig. 7 Pressure drops across the core during alternating injection. **a** Conventional foam. **b** Novel foam

every section. As early as 0.5 IPV, the strong foam propagated into Sect. 2 and then toward into Sect. 3 after 1.1 IPV. Much quicker foam propagation is attributed to the ability of the surfactant to dissolve in CO₂ without interference from water injection as well as inlet gas trapping. Foam collapsed when water saturation reached the critical value regionally. However, a huge amount of gas trapped in the core indicated by the residual pressure drops as high as 4 psi across the whole core is beneficial enough to the gas mobility control. Correspondingly, after gas breakthrough and weak foam propagation at 0.5 IPV, the strong foam developed in following sections drops the water saturation to 0.25 as early as 2.4 IPV and then levels off. This novel injection strategy really displays the superior surfactant transportation and foam propagation ability of this CO₂-soluble surfactant. In addition, the foam strength here in apparent viscosity was at least one magnitude higher than published data of other soluble surfactants (Xing et al. 2012; McLendon et al. 2014), which confirmed the superior capacity to stabilize the bubbles by the currently employed novel surfactant.

4.2 Simulation

4.2.1 Constant rate injection mode

4.2.1.1 Alternating injection From the gas production rate file (Fig. 10), early CO₂ breakthrough due to gravity segregation can be clearly observed at almost the same time for both types of foams. However, thereafter, the gas production rates differ significantly. For the conventional foam (zero partition coefficient), the gas rate abruptly increases and almost levels off quickly; while it decreases for the novel CO₂-soluble surfactant foam as the partition coefficient becomes nonzero. The distributions of gas saturation (Fig. 11a, b) in the reservoir at the end of injection

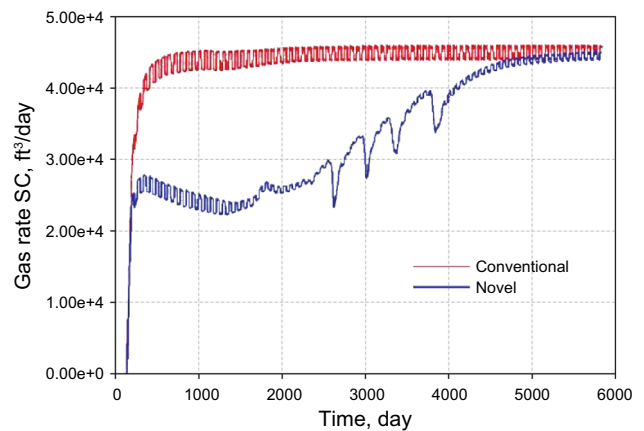


Fig. 10 Gas production rate of small slug size (36.5 days)

show that once gas reached the edge of the surfactant front at the top of the reservoir, it rapidly segregated upwards and reaches the production well in a thin override zone (Rossen and Renkema 2007). On the contrary, the novel foam increases the override zone dramatically even though the two types of foams gave the same gravity segregation length (R_g), which were read from profiles approximately as 130 ft. The tremendously different performances of the two foams essentially come from surfactant properties and can be seen on the concentration distribution profiles (Fig. 12a, b). There is a surfactant vacuum zone in the top layer for the conventional foam, while it exists only near the wellbore for the novel foam. The key reason of fluid segregation leading to the foam process losing efficiency is not only gas override but also surfactant slumping with water. Rossen and Renkema (2007) obtained the similar observation that surfactant has slumped toward the bottom of the reservoir and there was no surfactant ahead of the foam front at the top of the reservoir. The novel surfactant would be chased by the following gas slug and is delivered to the top layer with CO₂ override. Then, the gas mobility

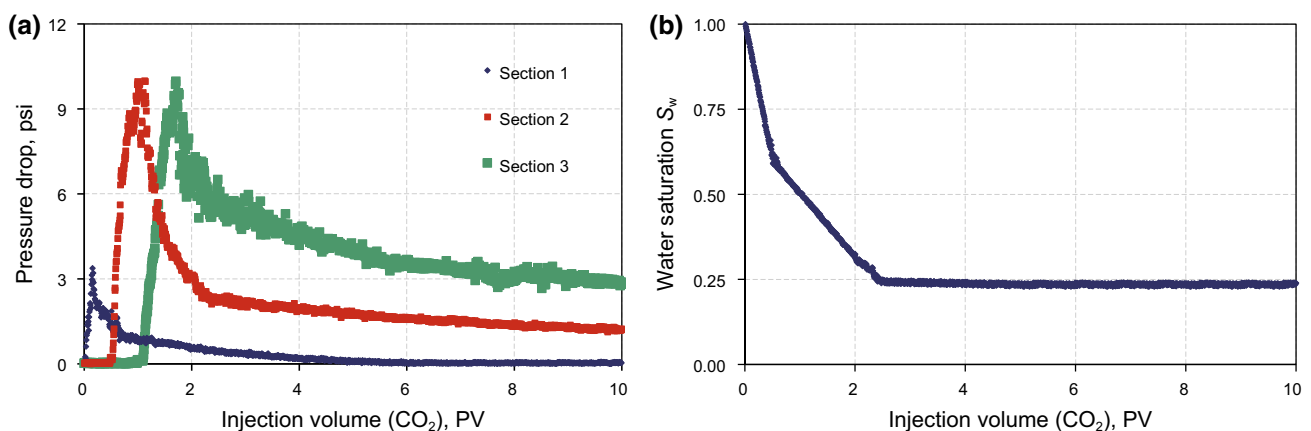


Fig. 9 Pressure drops across the core (a) and average water saturation in the core (b) during CO₂ continuous injection with dissolved CO₂-soluble surfactant

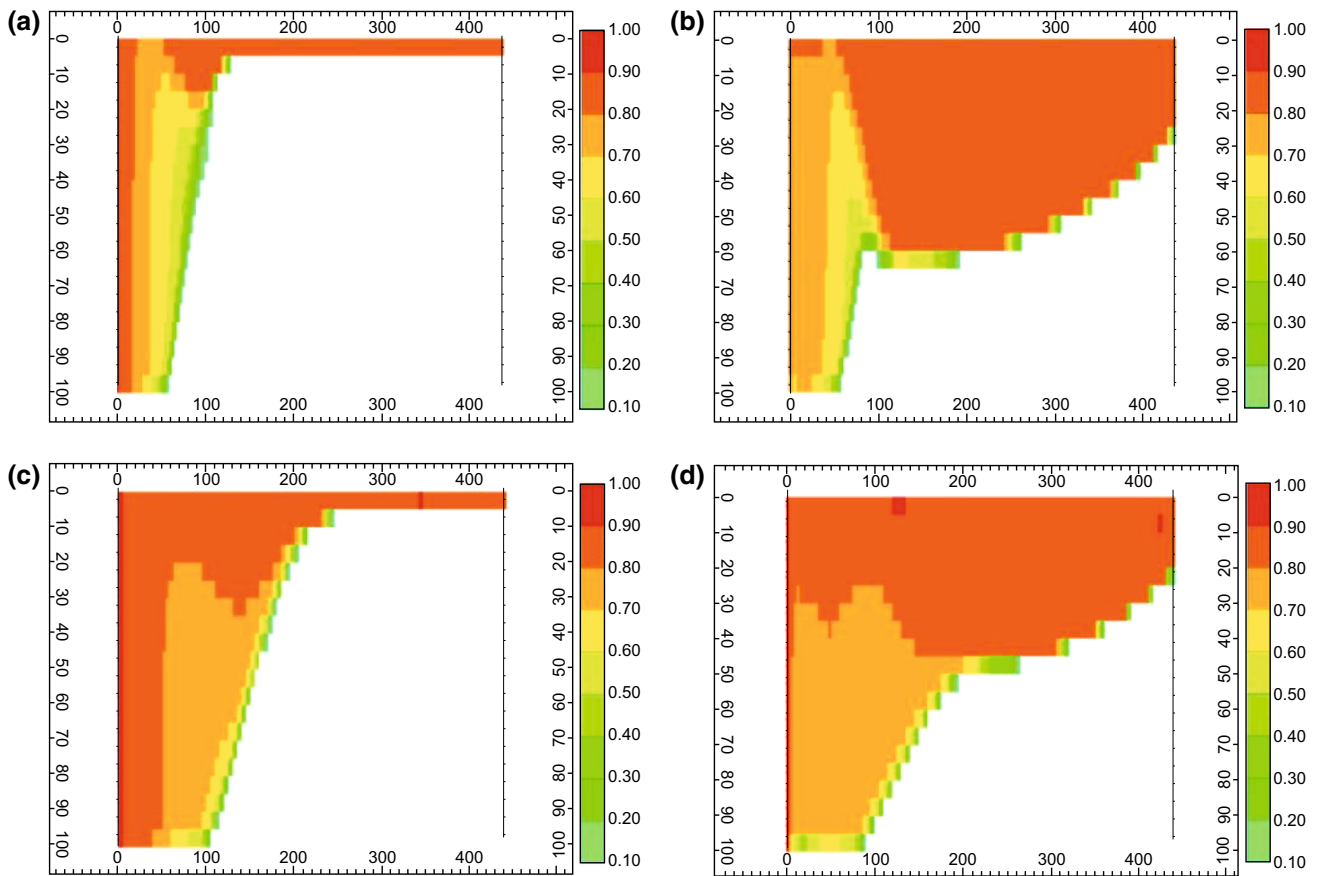


Fig. 11 Gas saturation of small slug size (36.5 days) for **a** CD1045, **b** novel surfactant and of larger slug size (182.5 days) for **c** CD1045, **d** novel surfactant during alternating injection

in the override zone has been reduced greatly and effective diversion occurred. Furthermore, this particular surfactant partitioning improves not only sweep efficiency, but also well injectivity with significantly reduced surfactant concentration near the wellbore. Here, one may have the suspicion that whether the superiority of the novel foam comes from the foam model effect. It is true that we employ the surfactant concentration in the water phase as the scale for gas mobility reduction in the simulation. Theoretically, we should supervise the concentration in the whole cell (*global*) because surfactant will act at the interface regardless of its partition in the gas phase. In reality, a comparison between corresponding plots (Figs. 12 vs. 13) tells us they display exactly the same trend except for the magnitude, which is attributed to the mass conservation and constant partition coefficient of injected fluids. Hence, in the following parts, we will only employ and illustrate the surfactant concentration in the aqueous phase.

With a larger injection cycle (182.5 days), for the conventional foam (Fig. 11a, c), an increase in the slug size significantly improves the vertical sweep efficiency by extending the distance R_g that the injected gas–water mixture flows before complete segregation but at the cost

of much lower injectivity (Ren et al. 2013). It was observed that the average bottom-hole pressure (BHP) of both foams increased with larger slug size (Ren et al. 2013). Indeed, the well bottom-hole pressure decreases for the novel foam over the conventional one (Fig. 14). It has been established that R_g increases with foam strength (i.e., reduced total relative fluid mobility, λ_{rt}) for the conventional foam as described by Eq. (2) (Rossen et al. 2006). Therefore, with higher injection pressure, the larger slug size yields stronger foam because of larger contact between the injected CO_2 and surfactant slugs. It is much clearer to observe the variation of R_g from Fig. 12a, c with the shrinkage of the low surfactant concentration zone in the top layers for the conventional foam. However, a comparison between Fig. 11b, d reveals that the novel foam is actually weaker with larger slug size as indicated by the overall reduction in the gas saturation. Different from the performance of CD1045, a larger slug size expands the low surfactant concentration area near the wellbore for the novel foam (Fig. 12b, d), which tends to lower the injection pressure and may decrease the sweep efficiency. Reservoir pressure distribution, as shown in Fig. 15, can be a more direct way to correlate surfactant transport with foam

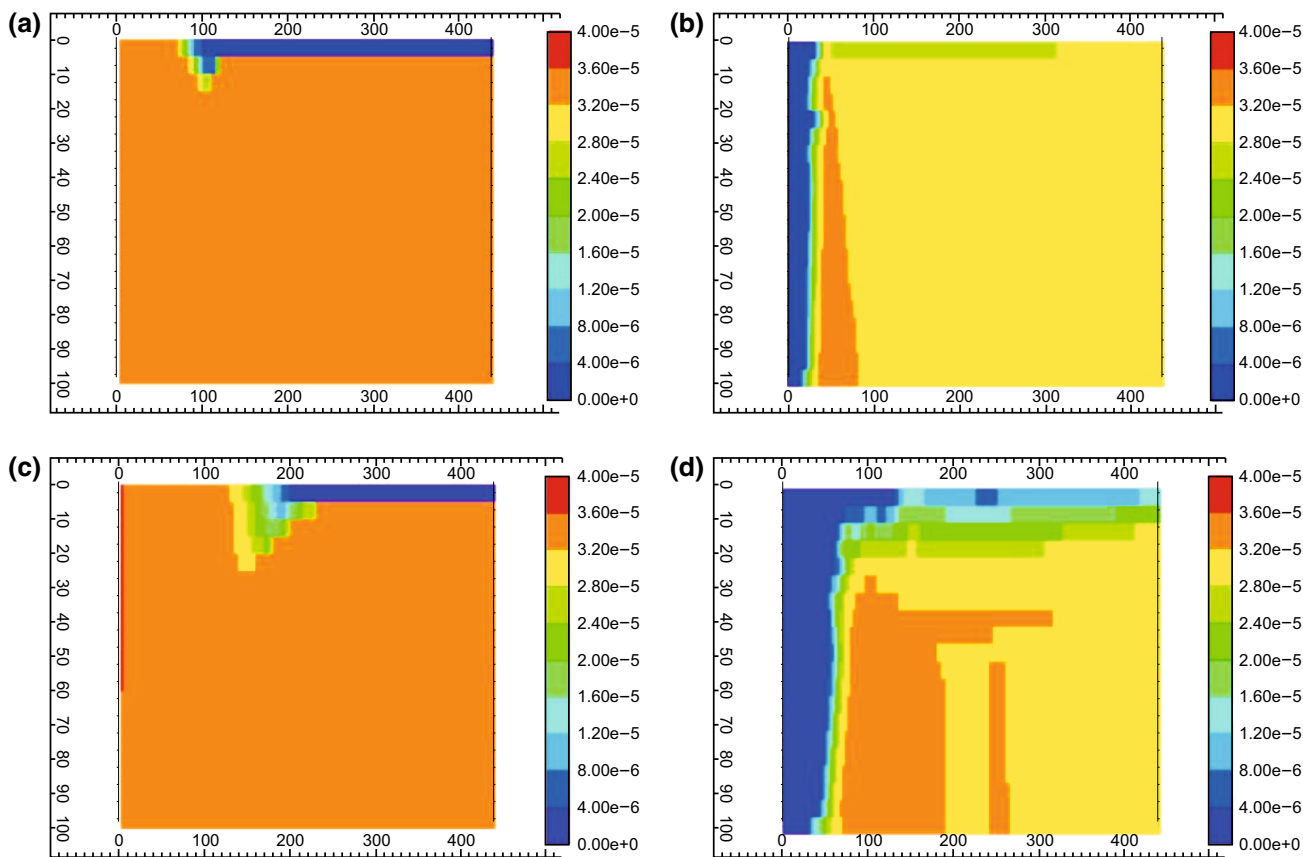


Fig. 12 Surfactant concentration in the water phase of small slug size (36.5 days) for **a** CD1045, **b** novel surfactant and of larger slug size (182.5 days) for **c** CD1045, **d** novel surfactant during alternating injection

propagation and fluid redistribution. For the conventional surfactant, the high pressure gradient is concentrated only within the near-wellbore region and expands somewhat from the wellbore as the fluid cycle increases (Shan and Rossen 2004). However, it spreads much further into the reservoir for CO₂-soluble surfactant indicating by a more even pressure gradient distribution. The variations of CO₂ storage and R_g with slug size are summarized in Table 3 as well as Fig. 16. With slug size increasing, the gravity segregation lengths do enlarge for both types of foams. However, the sweep efficiency varies differently, 11% reduction for the novel foam and 111% improvement for the conventional one. Therefore, we confirm the previous conclusion for the conventional foam the larger slug size was beneficial to the foam process for cylindrical homogeneous reservoirs (Shan and Rossen 2004; Rossen and Shen 2007; Rossen and Renkema 2007). For the novel foam, insensitivity to injected slug size gives less restriction for operation. With CO₂-soluble surfactant, the contradiction between gravity segregation length and CO₂ storage tells us again that R_g is only one criterion for fighting gravity segregation and not the sufficient condition.

$$R_g = \sqrt{\frac{Q}{\pi k_z (\rho_w - \rho_g) g \lambda_{rt}^m}} \tag{2}$$

4.2.1.2 Co-injection

(1) Water and gas injection through the same intervals (SIAP and SIPP)

Figure 17 shows gas production rates for two different simultaneous injection strategies with distinct perforation locations. For the full completion (SIAP), both the novel and conventional foams give unsatisfactory performances even though the former is fluctuating to approach the steady state after gas breakthrough in a short time. With partial completion in the lower interval (SIPP), the improvement in the conventional foam is almost unnoticeable, while a distinct reduction in gas production is showed by CO₂-soluble surfactant foam. More clear comparisons can be seen in gas saturation distributions (Fig. 18). For SIAP, the injected gas concentrates highly in the top layers. The huge difference between gas and water mobility contributes to the poor performance for both foams. Eventually, from this point of view, the novel surfactant makes the situation worse because the gas

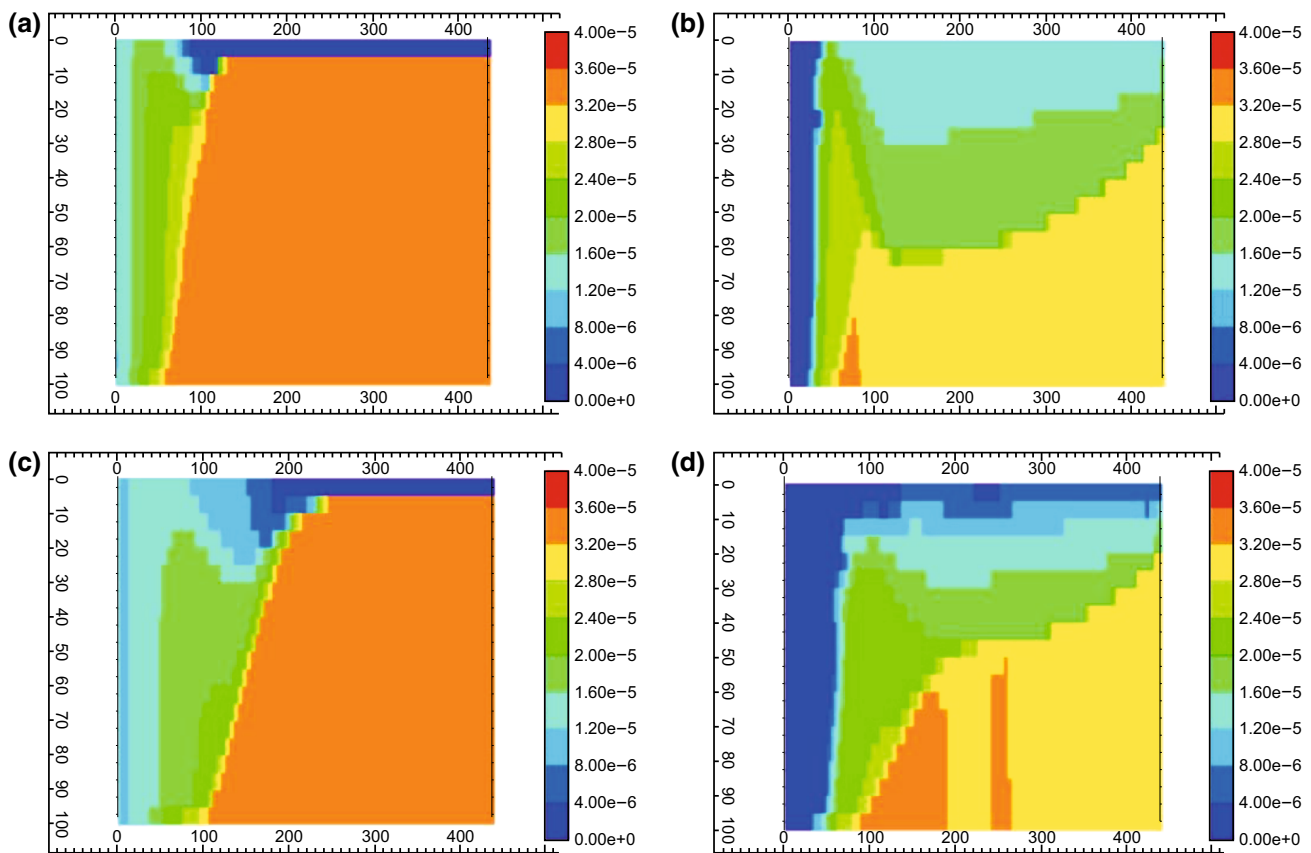


Fig. 13 Global surfactant concentration of small slug size (36.5 days) for **a** CD1045, **b** novel surfactant and of larger slug size (182.5 days) for **c** CD1045, **d** novel surfactant, during alternating injection

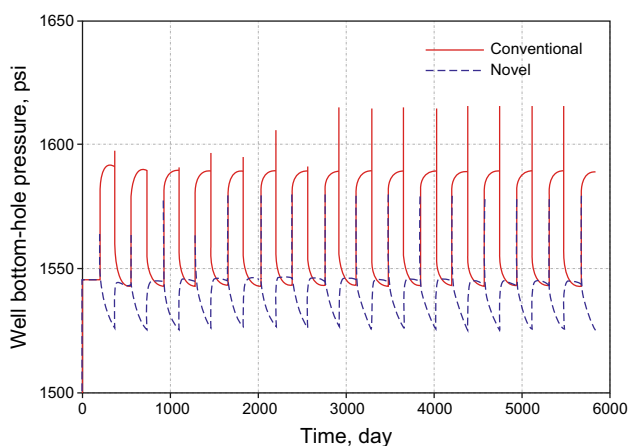


Fig. 14 Gas well BHP of large slug size (182.5 days)

extraction effect CO_2 -soluble surfactant decreases the surfactant concentration on the gas escape path further. Even though the chased surfactant is transported to the top layer far from the injector, now it fails to reduce the gas mobility because too much gas flow results in a very low surfactant concentration, as shown in Fig. 19a, b, which fails the effective gas diversion. On the other hand, for

SIPP, injection from the lower part does improve gas storage for the conventional foam near the wellbore (Fig. 18c). A conventional aqueous soluble surfactant will slump with water and a lack of ability to migrate to the top layer will not heal the surfactant scarce zone (Fig. 19c). Oppositely, the novel foam highly expands the override zone vertically (Fig. 19d) since the increased water and gas contact will retain more CO_2 -soluble surfactant in the upper zone and the gas escape path does not exist anymore (Fig. 19d). Meanwhile, we confirm that the partial perforation does significantly increase the bottom-hole pressure relative to the full completion (Rossen et al. 2006; Rossen and Shen 2007; Jamshidnezhad et al. 2008b) even though the novel foam always gives a lower value, as shown in Fig. 20. In addition, compared with alternating injection, simultaneous injection does lower the injectivity for the conventional foam (Rossen et al. 1995) while this problem has been greatly mitigated with the novel foam (SIAP) even though the sweep efficiency is relatively poor. The pressure distribution in the reservoir, Fig. 21, provides a direct evidence for injection strategy screening. High pressure gradient compresses near the wellbore for both completion schemes although the novel foam is still

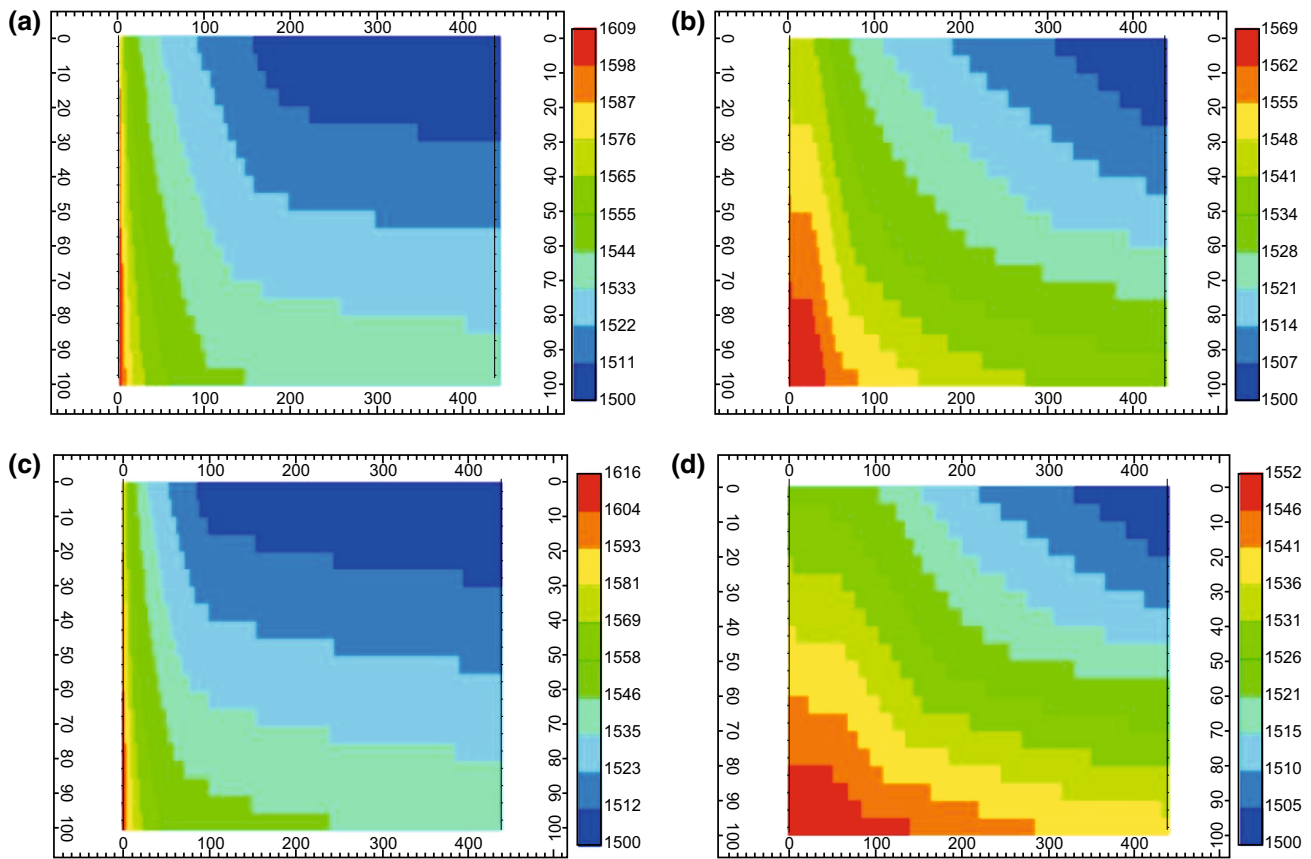


Fig. 15 Pressure distribution of small slug size (36.5 days) for **a** CD1045, **b** novel surfactant and of larger slug size (182.5 days) for **c** CD1045, **d** novel surfactant during alternating injection

Table 3 CO₂ storage and gravity segregation length

	CO ₂ storage, 10 ⁷ scf		R _g , ft	
	36.5-day slug size	182.5-day slug size	36.5-day slug size	182.5-day slug size
Novel	7.36	6.54	130	200
Conventional	1.16	2.45	130	165

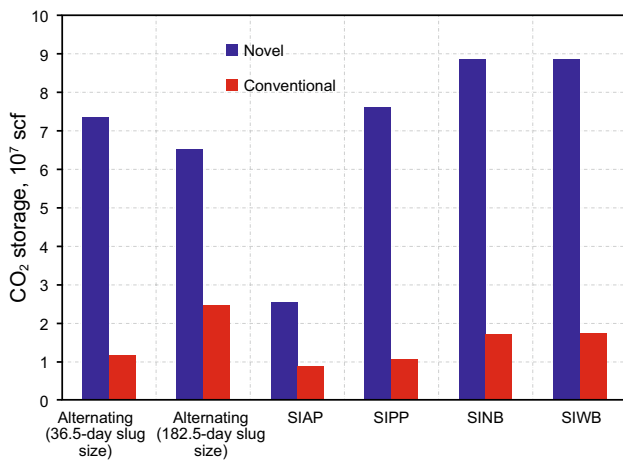


Fig. 16 Summary of CO₂ storages for alternating and simultaneous injection with constant rate injection mode

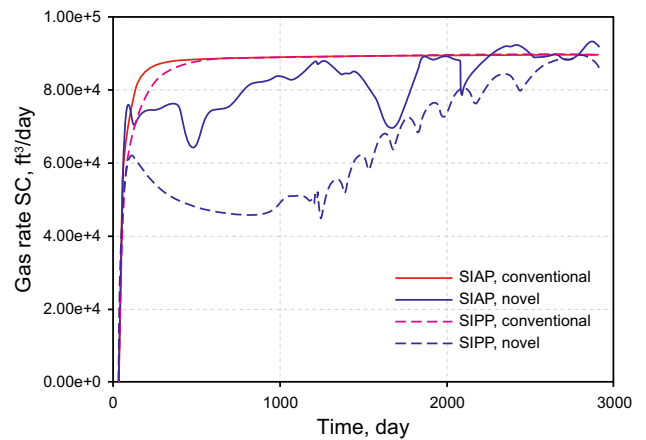


Fig. 17 Gas production rate during SIAP and SIPP

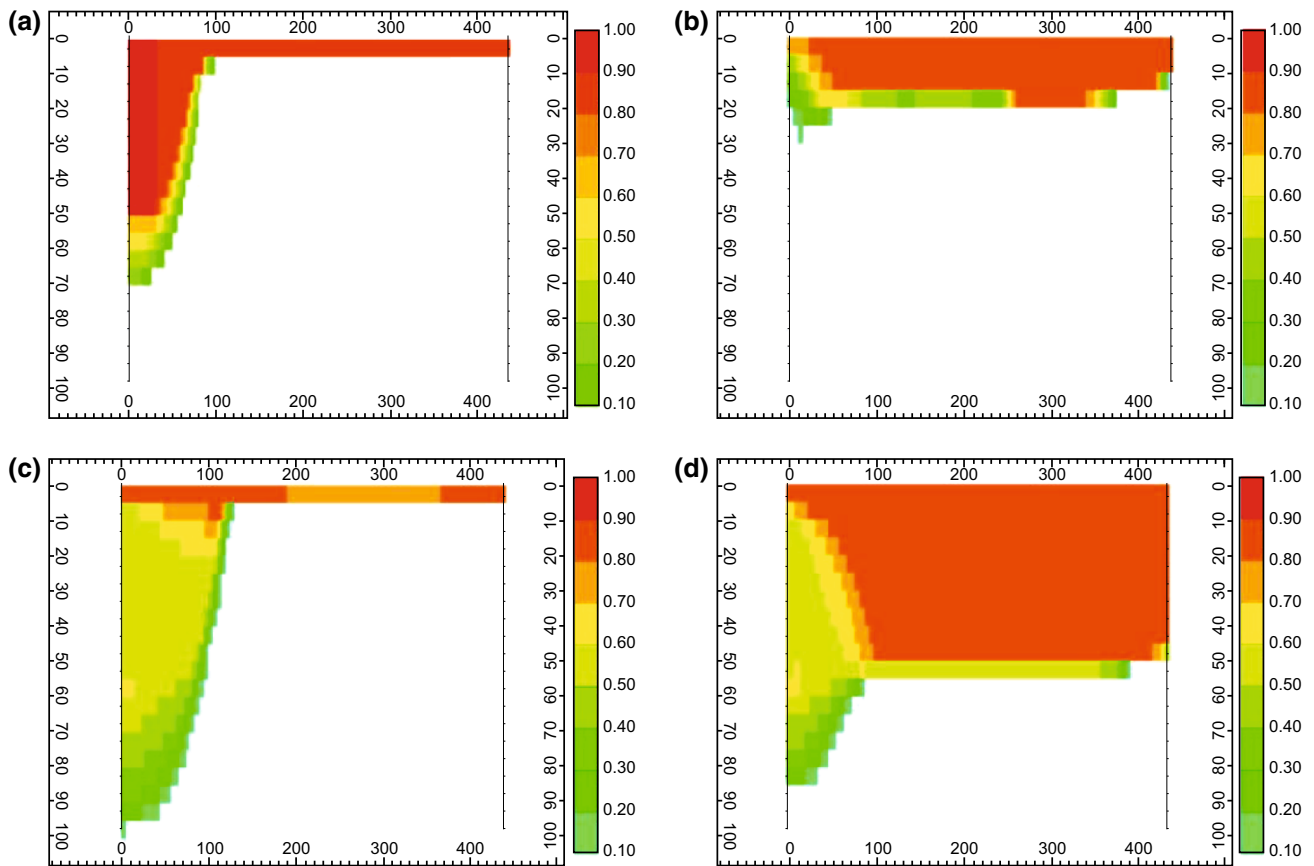


Fig. 18 Gas saturation during SIAP of **a** convective foam and **b** novel foam and during SIPP of **c** conventional foam and **d** novel foam

superior over the conventional one with respect to sweep efficiency and injectivity. This is in accordance with the previous conclusion that relative to SAG with constant injection rate, a foam process with continuous foam injection performs even worse, because most of the well-to-well pressure drop was dissipated in the near-well region (Shi et al. 1998; Shan and Rossen 2004; Rossen and Shen 2007). The results in this case tell us gas override takes precedence in importance over water slumping in fighting gravity segregation (Shan and Rossen 2004).

Table 4 summarizes CO_2 storage (Fig. 16) and gravity segregation length for SIAP and SIPP. It is obvious that the novel foam gives much higher sweep efficiency than the conventional one. Here, we do confirm the close R_g with alternating injection for SIPP, but not for SIAP, which is expected as the cycle size decreases (Shan and Rossen 2004). In addition, we do not reach the conclusion that R_g for constant rate injection is not sensitive to the simultaneous injection of gas and water into either a partially (SIPP) or a fully completed well (SIAP) (Rossen et al. 2006; Rossen and Shen 2007; Jamshidnezhad et al. 2008b).

(2) *Injection of water into the top part and gas into the bottom part (SINB and SIWB)*

Figure 22 shows the gas production rates for another two different simultaneous injection strategies with water injection through the top and gas into the bottom (SINB and SIWB). Except for injectivity (Fig. 23), it is hard to tell the difference between partial and full completions as regards of gas production rate, gas saturation, and surfactant distribution for both foams. Therefore, only plots of SINB are shown for those parameters. For the conventional foam, again, injectivity reduction is observed as a typical characteristic of the partial completion. On the other hand, the novel foam really reduces the difference caused by perforation locations, but not to the same extent as in the above two strategies (SIAP and SIPP, Fig. 20). The gas–water mixed zones, as shown in Fig. 24, do not expand vertically for the conventional foam, while opposite is observed for the CO_2 -soluble surfactant foam. The injection of water above gas increases the travel distance for both gas and water in the vertical countercurrent flow (Rossen et al. 2006) which is in turn resisted by foam

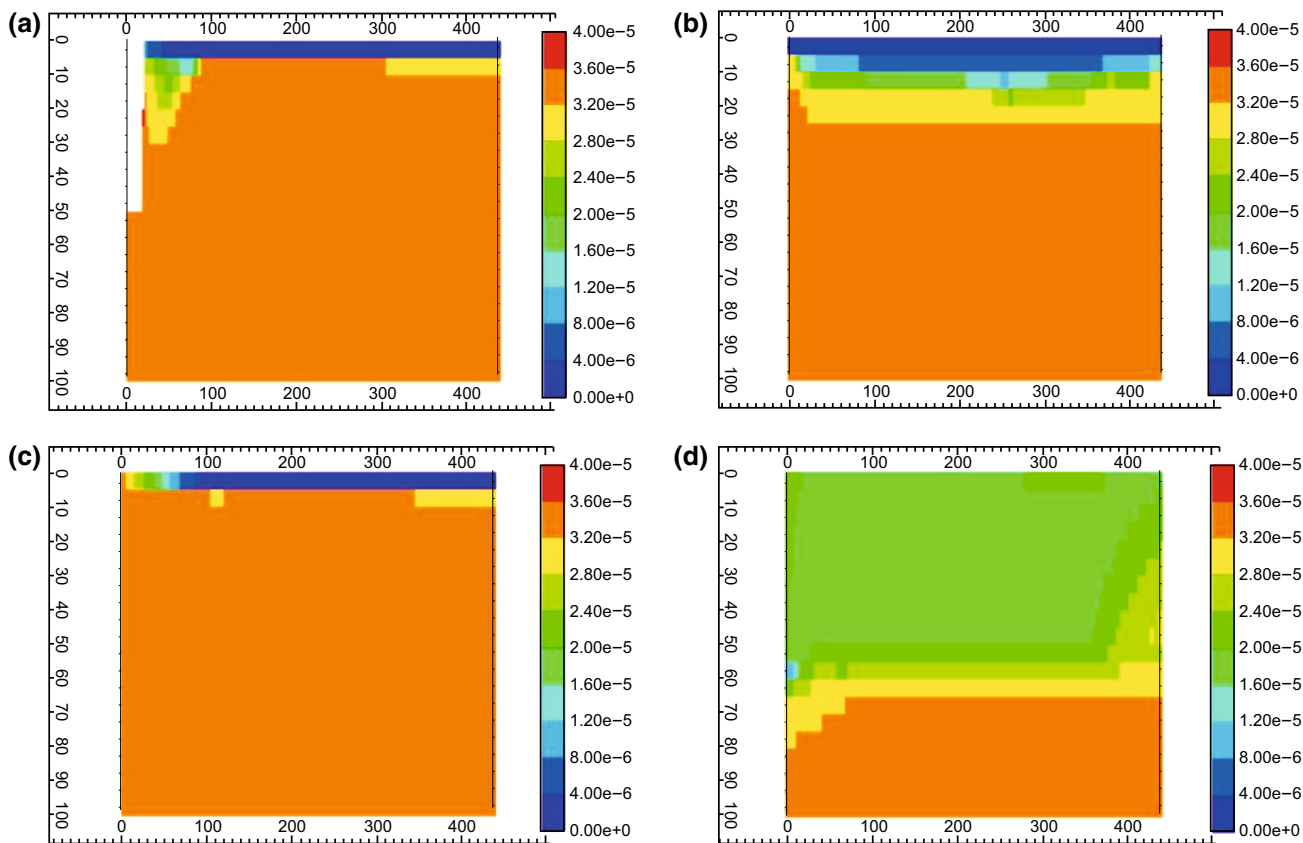


Fig. 19 Surfactant concentration during SIAP of **a** convective foam and **b** novel foam and during SIPP of **c** conventional foam, **d** novel foam

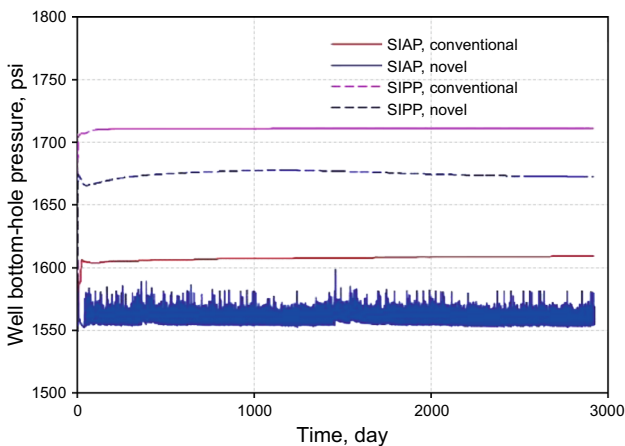


Fig. 20 Well bottom-hole pressures during SIAP and SIPP

formation. The advantage is further enhanced with the CO₂-soluble surfactant as this injection strategy allows more surfactant to be carried with CO₂ into the override zone. As a result, better foam propagation in the upper part of the reservoir can be achieved. This is illustrated by the surfactant concentration distribution (Fig. 25) and pressure

distribution in the reservoir (Fig. 26). Now, relative to the conventional foam, the novel surfactant extends the high pressure gradient much further into the reservoir with more even pressure distribution.

Table 4 also summarizes CO₂ storage (Fig. 16) and gravity segregation lengths for those two separate injections. It is obvious that the novel foam still gives much higher sweep efficiency than the conventional one. We do achieve the same R_g for SINB and SIWB as well as the higher injection pressure for the latter (Rossen et al. 2006; Rossen and Shen 2007; Jamshidnezhad et al. 2008b). However, the sweep efficiency improvement was not remarkable, particularly for the novel foam. Relative to water and gas injection through the same intervals (SIAP and SIPP), the distance to the point of complete segregation R_g increases by a factor of about 1.5 and higher injectivity (Figs. 20, 23) has been achieved for separate injection (SINB and SIWB). This result agrees with the theoretical prediction of R_g as a function of water fractional flow reported in the literature (Rossen et al. 2006; Rossen and Shen 2007). From above analysis we can find, for novel foam, gravity segregation length is a less precise representative parameter of sweep efficiency.

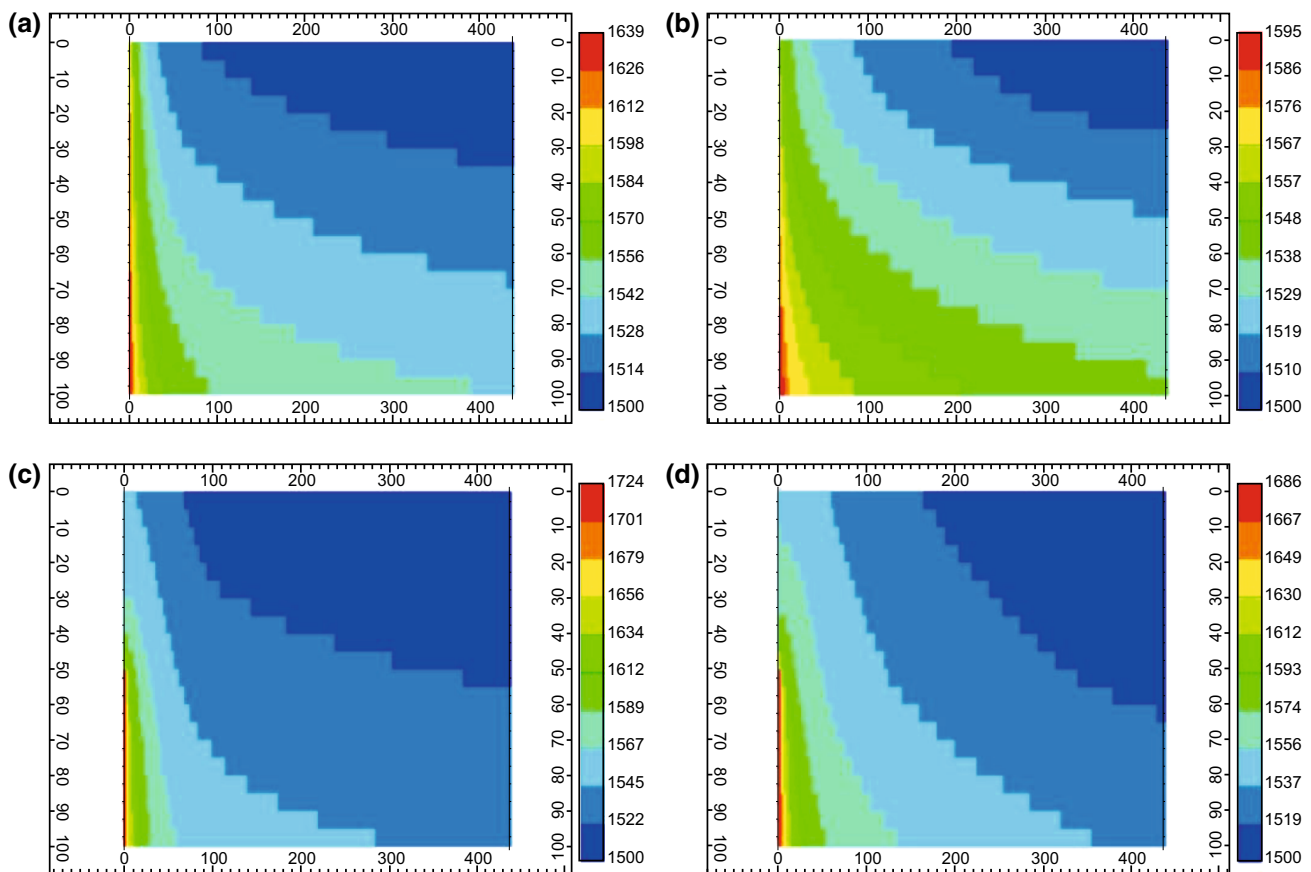


Fig. 21 Pressure distribution during SIAP of **a** convective foam and **b** novel foam and during SIPP of **c** conventional foam, **d** novel foam

Table 4 Comparison of CO₂ storage and gravity segregation length among alternating and simultaneous injection

	CO ₂ storage, 10 ⁷ scf		R_{g^*} , ft	
	Novel	Conventional	Novel	Conventional
Alternating injection (36.5-ay slug size)	7.36	1.16	130	130
SIAP	2.54	0.874	54	30
SIPP	7.61	1.06	115	115
SINB	8.9	1.73	215	190
SIWB	8.9	1.74	215	190

4.2.2 Constant pressure injection mode

The performance difference between novel and conventional foams is illustrated below. Also, we will address the validation of the previous conclusion that this mode was more efficient than the constant rate mode and whether this is still valid for the novel foam (Shan and Rossen 2004)

4.2.2.1 Alternating injection Let us look at alternating injection with a 36.5-day slug size first. In earlier studies (Shan and Rossen 2004; Rossen et al. 2006; Rossen and Shen 2007; Rossen and Renkema 2007; Kloet et al. 2009), conservation of injection fluids including water, gas, and surfactant was not maintained between two injection

modes, which causes the quandary that whether the superiority of constant pressure mode comes from more injected surfactant over constant rate mode. Therefore, we try to pursue the conservation through trial and error on injection pressure. However, owing to different injectivity between novel and conventional foams, we decide to use the values close to those for the conventional one for the first manipulation. 1581 psi for the gas well and 1547 psi for the water well were determined through strictly equalizing amounts of injection phases for the conventional foam between two modes. Then, the same pressures were used for the novel foam. It is straightforward that much more fluid will be injected for the novel foam owing to higher injectivity, as shown in Fig. 27a. The CO₂ storages are

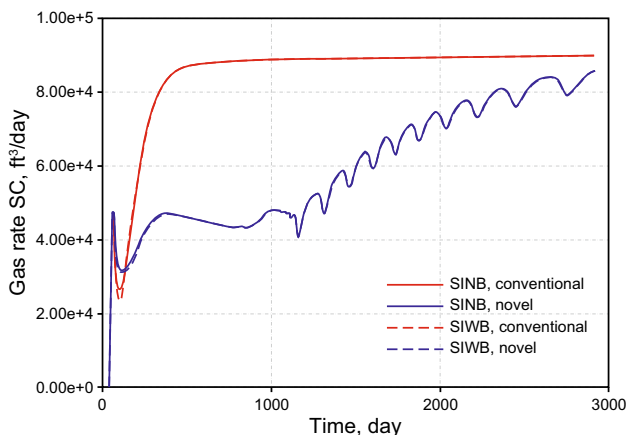


Fig. 22 Gas production rate during SINB and SIWB

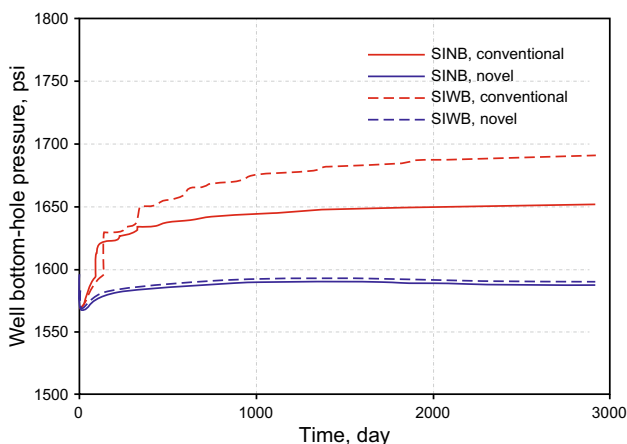


Fig. 23 Well bottom-hole pressure during SINB and SIWB

listed in Table 5, which are improved 3.6% and 50.7% for conventional and novel foams, respectively, relative to the constant rate mode. For the conventional foam, the constant pressure mode can increase the injection rate when the foam near the wellbore becomes weak owing to water

saturation approaching the critical value (Rossen et al. 1995); thus with relatively high mobility ahead of and behind the displacement front, a pressure-constrained SAG process can force the entire reservoir pressure drop into the region of low mobility at the displacement front, i.e., more even pressure drop distribution is expected instead of most of them dissipating in a short distance. However, our results show that the improvement is very limited, with respect to gas saturation (Fig. 28a), surfactant concentration (Fig. 29a), and pressure distribution (Fig. 30a). All of those are extremely similar to the results before with the constant rate mode (Figs. 11a, 12a). Hence, we deduce the injection mode may not be the crucial parameter as long as injection mass conservation is honored. On the other hand, from the point view of sweep efficiency, alternating injection with constant pressure mode tends to amplify the superiority of the novel foam over the conventional one, characterized by a vertically expanded gas saturation profile (Fig. 28b), uniform surfactant distribution (Fig. 29b), and much deeper extended high pressure gradient (Fig. 30b), even though more gas has been produced (Fig. 31a). In addition, it seems that the constant pressure mode does able the enhancement of the sweep efficiency tremendously for the novel foam (Figs. 11b, 28b), which deserves further discussion below. Meanwhile, unequal amount of gas injection requires us to employ another parameter, CO₂ utilization ratios, for the economic consideration, which are also listed in Table 5. Therefore, there is no question that for alternating injection, constant pressure injection mode is beneficial to conventional foam with respect to both sweep efficiency and CO₂ utilization ratio even though the improvement is trivial. For the novel foam, operators need to balance the extra profits from 50% sweep efficiency improvement against the ascending injection cost from 29% deducted gas utilization even though it is still more than four times higher than that of conventional foam.

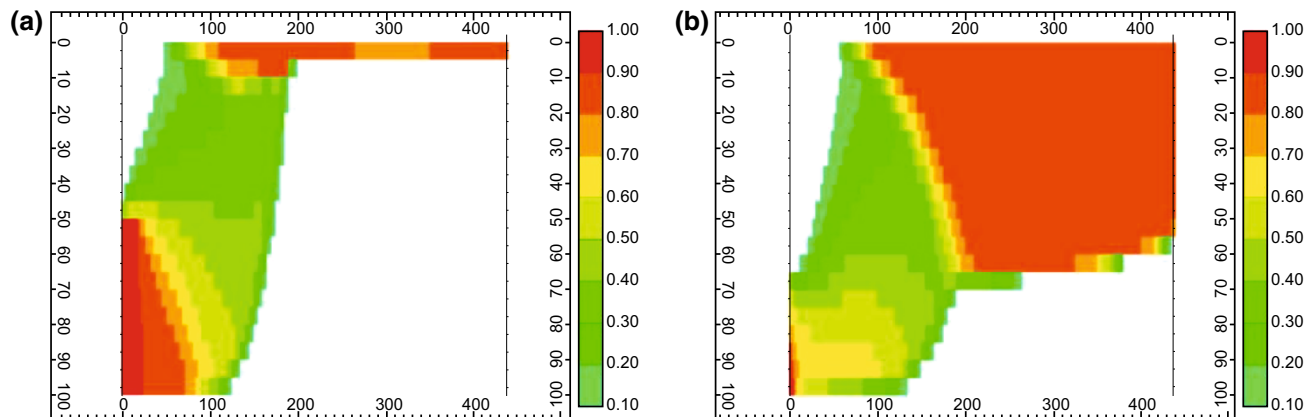


Fig. 24 Gas saturation during SINB of a conventional foam and b novel foam

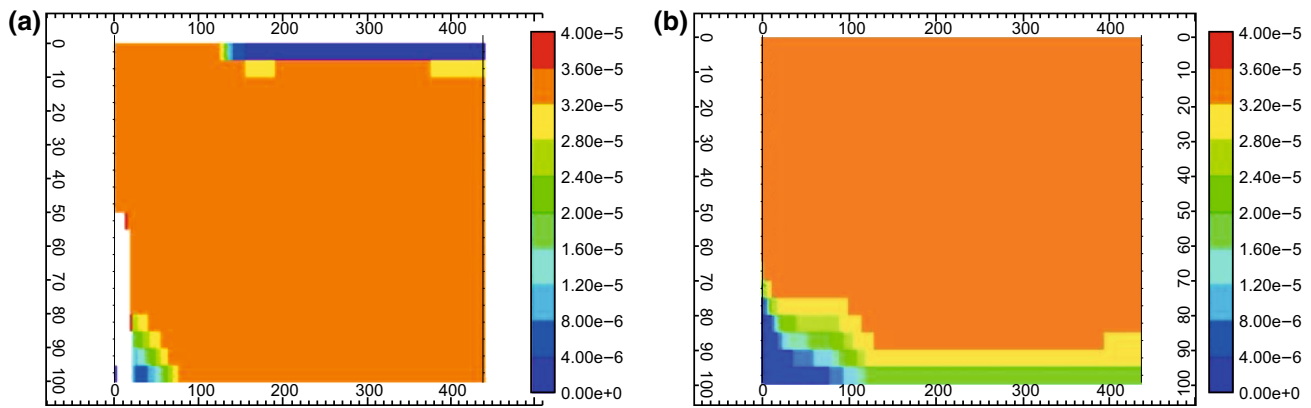


Fig. 25 Surfactant concentration during SINB of **a** conventional foam and **b** novel foam

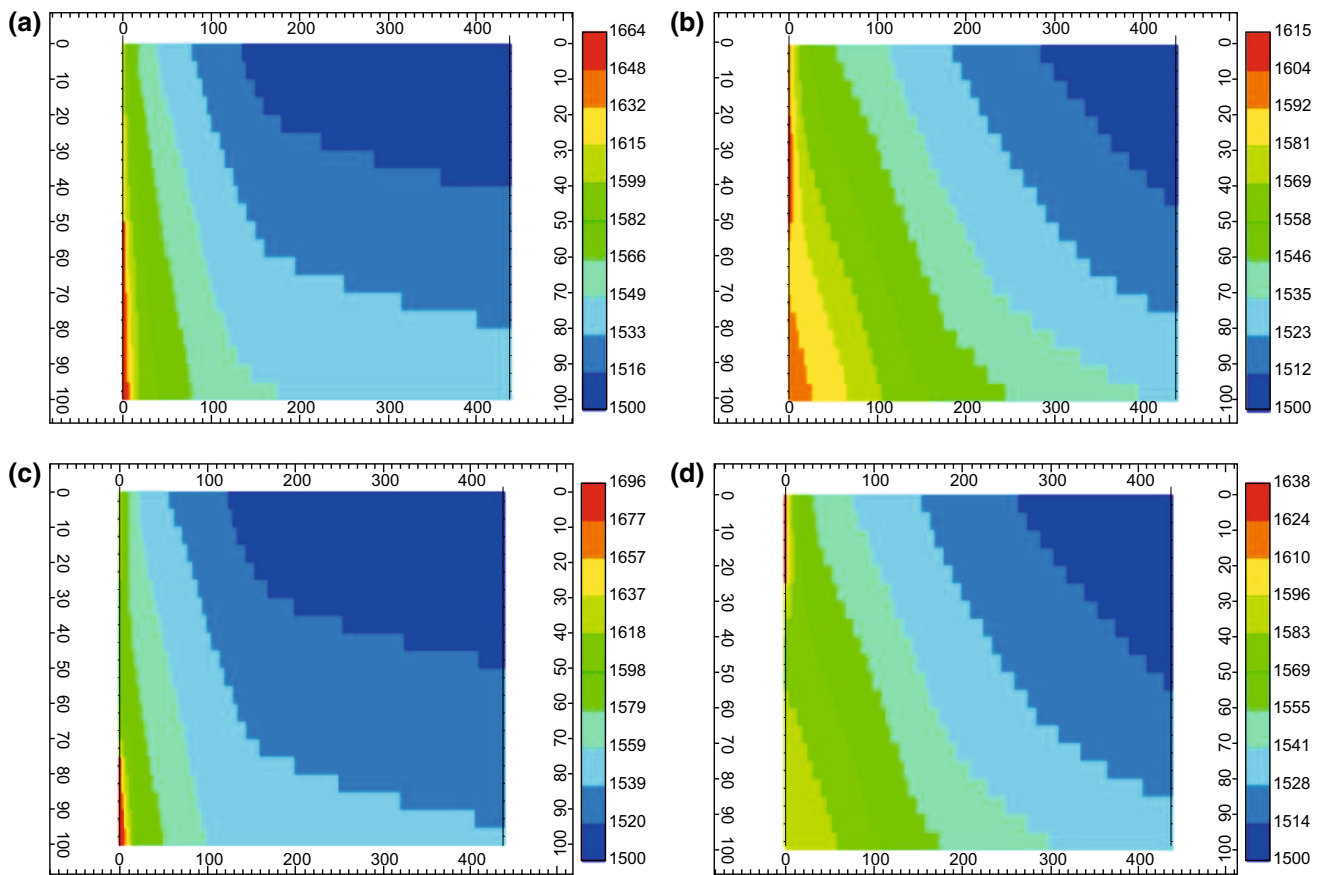


Fig. 26 Pressure distribution during SINB of **a** conventional foam and **b** novel foam and during SIWB of **c** conventional foam, and **d** novel foam

Now, let us address the remaining question above that whether the significant improvement in novel foam performance is attributable to the constant pressure injection mode. We follow the manipulation above to search the lower injection pressures through pursuing injected fluid conservation for the novel foam at 36.5-day slug size with constant rate mode, saying 1548 psi for the gas well and 1553 psi for the water well. The CO_2 storage and gas utilization ratio are also listed in Table 5, which are just

slightly higher than those in the constant rate mode. This is consistent with the deduction we did for the conventional foam. Thus, the improved CO_2 storage and reduced CO_2 utilization above just result from more fluid injections. In other words, for both types of foams, the injection mode is of less importance as long as a close average injection rate or pressure is fulfilled.

In the constant rate mode section, we already concluded that the novel foam was insensitive to the slug size for

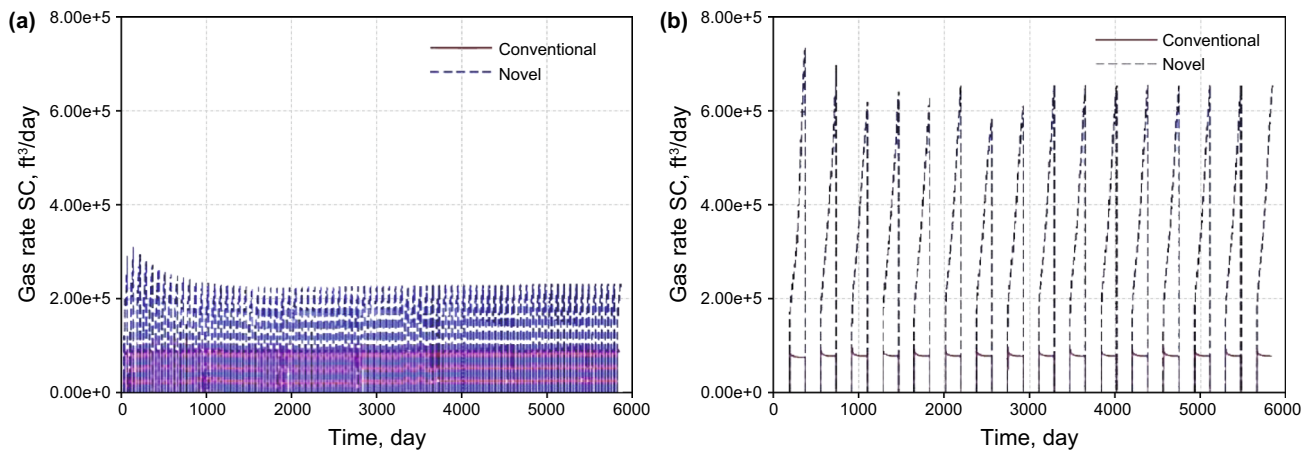


Fig. 27 Gas injection rate of alternating injection under constant pressure constraint for **a** 36.5 days and **b** 182.5 days

Table 5 Comparison of CO₂ storage and utilization ratio for constant rate and pressure injection modes for alternating injection

	CO ₂ storage, 10 ⁷ scf				CO ₂ utilization ratio					
	Constant rate		Constant pressure		Constant rate		Constant pressure			
	36.5 days	182.5 days	36.5 days	182.5 days	36.5 days	182.5 days	36.5 days	182.5 days		
Novel	7.36	6.54	11.1	7.68	12.2	0.28	0.249	0.199	0.289	0.105
Conventional	1.16	2.45	1.2	–	2.28	0.044	0.0933	0.046	–	0.096

alternating injection even though smaller size held the leading position slightly. Now, we extend the above discussion to the constant pressure constraint. 1581 psi for the gas well and 1547 psi for the water well are still employed. It is observed that larger slug size increases the novel foam gas injection rate and enlarges the contrast between two types of foams (Fig. 27) since the novel foam will lower the injection pressure further with larger slug size. In turn, similar trends are expected for gas production rates (Fig. 31). The CO₂ storage and utilization ratios are listed in Table 5. For the conventional foam, it is obvious that larger slug size is preferred, indicated by the enhancement of sweep efficiency and utilization efficiency up to 90% and 100%, respectively, relative to smaller slug size. Hence, there comes the previous conclusion that the optimal injection strategy for overcoming gravity override with foam in a homogeneous reservoir is alternating injection of separate, large slugs of gas and liquid at a fixed, maximum-allowable injection pressure (Shan and Rossen 2004; Rossen and Renkema 2007). Meanwhile, if we examine the corresponding cases for two injection constraints with the same slug sizes under conservation of injection fluids, analogous improvements are present. Especially, the gas

saturation profile (Fig. 28c), surfactant concentration (Fig. 29c), and pressure distribution (Fig. 30c) are almost identical to those under constant rate constraints (Figs. 11c, 12c). Therefore, again, the injection constraint is really of less importance and the performance of the novel foam is overwhelming. With respect to sweep efficiency, we prove the novel foam is insensitive to the slug size with only 10% enhancement evidenced by the further vertical expanded override zone (Fig. 28d) and deeper extension of high pressure gradient (Fig. 30d). However, again, this costs a 47% reduction in CO₂ utilization efficiency indicated by the rocketing gas production rate (Fig. 31b) and low surfactant concentration zone in the upper layers (Fig. 29d). Therefore, for the novel foam, the sweep efficiency is a monotonic function of injection rate or pressure, but the gas utilization ratio could demonstrate a parabolic shape.

4.2.2.2 Water injection through the top part and gas into the bottom part (SINB) Similar to the manipulation above, we also looked at the injection pressures through trial and error to pursue the conservation of injected fluids for the conventional foam, 1608 psi for a gas well and 1598 psi for a water well; then, apply them to the novel

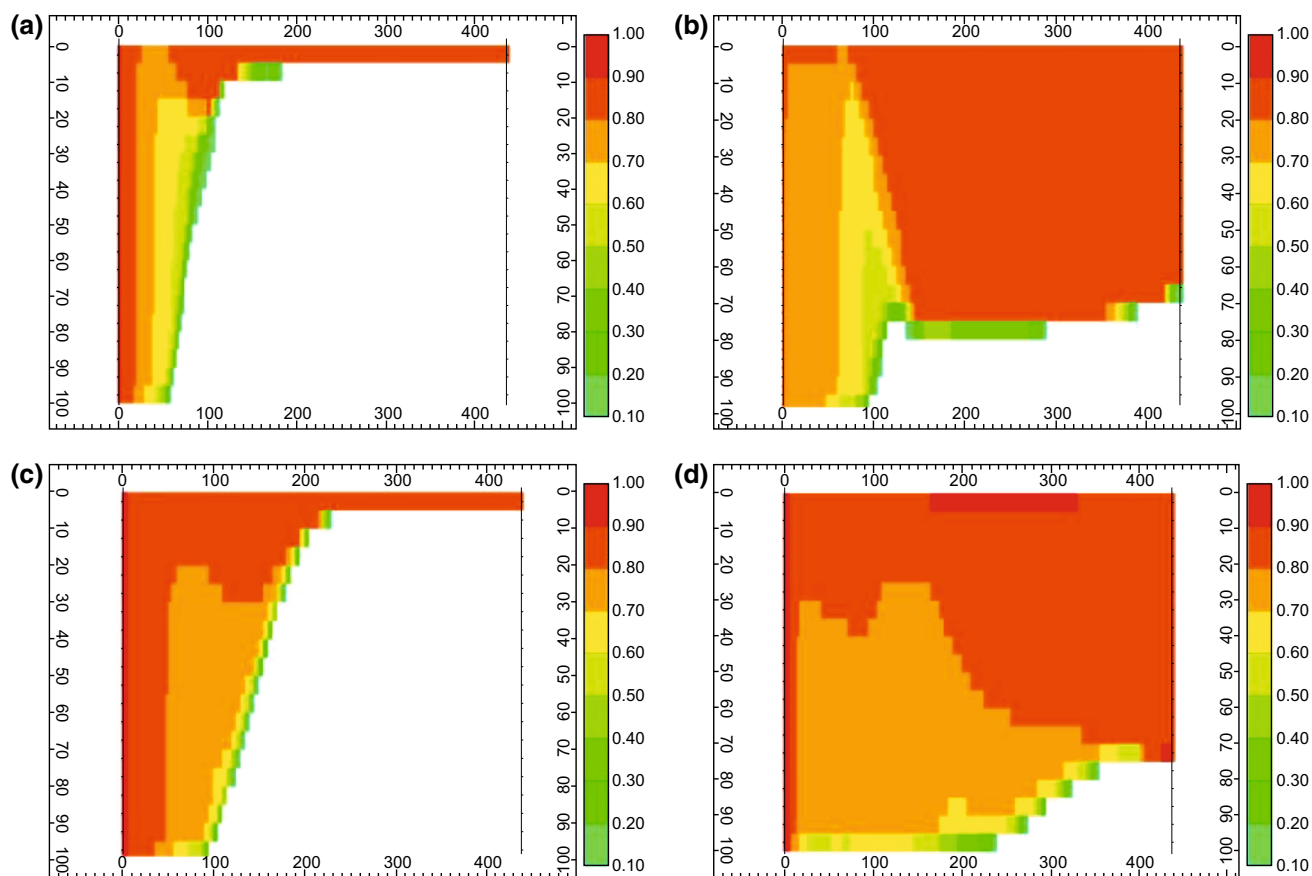


Fig. 28 Gas saturation of small slug size (36.5 days) for **a** CD1045, **b** novel surfactant, and of larger slug size (182.5 days) for **c** CD1045, **d** novel surfactant during alternating injection under constant pressure constraint

foam. The CO₂ storage and utilization ratio are listed in Table 6. A much higher gas injection rate and delayed increasing production rate (Fig. 32) indicate the higher injectivity and better efficiency for the novel foam. It is obvious that the novel foam outperforms the conventional one significantly, indicated by the extreme vertically expanded override zone (Figs. 33, 34), better surfactant transportation in the override zone (Figs. 35, 36) and more deeply extended high pressure gradient (Figs. 37, 38). A low surfactant concentration zone near the gas injector at the bottom characterizes the CO₂ partitioning ability of the novel surfactant. Similarly, the constant pressure constraint does tend to amplify the contrast between two types of foams with respect to CO₂ storage even though the CO₂ utilization ratio of the novel foam drops. It is clear that the comparison between two injection modes for the conventional foam tells us the constant pressure mode gives a little bit worse performance with close distributions of gas saturation (Figs. 24a, 33) and surfactant concentration (Figs. 25a, 35). This is not consistent with prior conclusions (Shi et al. 1998; Shan and Rossen 2004; Rossen et al.

2006; Rossen and Renkema 2007; Jamshidnezhad et al. 2008b) that regardless of co-injection or SAG, relative to the constant rate injection, the constant pressure injection can overcome gravity override better and obtain pressure distribution more evenly, i.e., most of the fixed pressure drop between wells is focused on the displacement front, with maximum suppression of the gravity effect. This discrepancy could be attributed to the different initial reservoir conditions made here. Most of the prior conclusions we mentioned up to now are based on the postulation that the reservoir is initially saturated with surfactant (Rossen et al. 1995; Shi et al. 1998; Shan and Rossen 2004), which means that these studies applied only to gravity override within the region swept by surfactant and slumping of the surfactant slug is not examined. In this study, no surfactant is present in the reservoir initially, which is more practical. Therefore, even though the constant pressure constraint tends to force the pressure drop at the displacement front (Rossen et al. 1995), it may give worse side effects for the same reason. The injection rates response (Fig. 32) gives some clues. Before enough

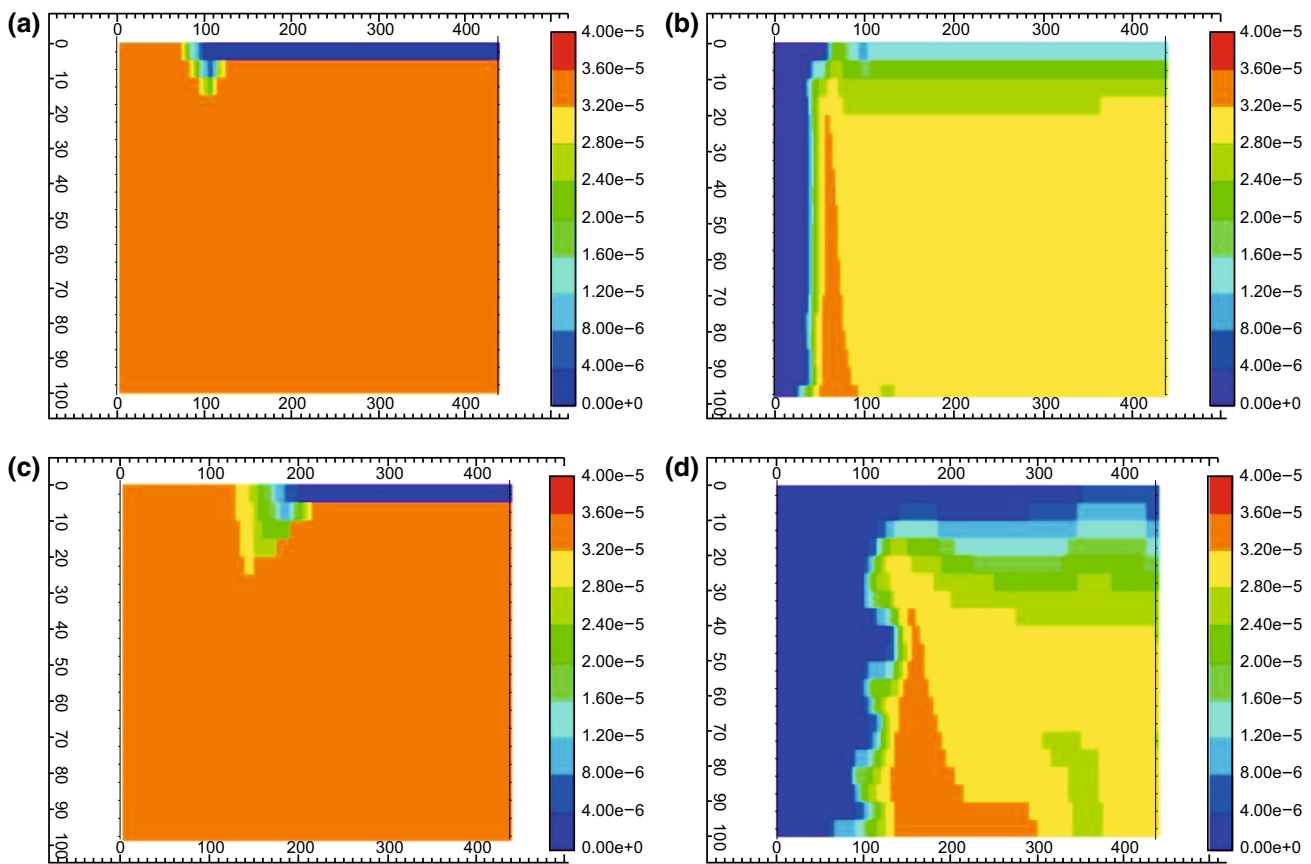


Fig. 29 Surfactant concentration of small slug size (36.5 days) for **a** CD1045, **b** novel surfactant, and of larger slug size (182.5 days) for **c** CD1045, **d** novel surfactant during alternating injection under constant pressure constraint

resistance presents ahead of the gas front, the injection rate rockets to a high level even though we employ the lower injection pressure relative to those under the constant rate constraint (Fig. 23). Then, it decreases to the similar value (90,000 scf/day) as the strong foam has been built up in the reservoir. The only advantage we can view here is the deeper extended high pressure gradient (Figs. 37, 26a).

Similar to our discussion above, with higher injection pressure, or much more fluid injected relative to the constant rate mode, CO₂ storage for the novel foam seems to significantly improve with a reduction of 58% in CO₂ utilization efficiency, even though the pressure gradient distribution is almost piston-like (Figs. 38, 26b). Therefore, to maintain conservation of injection fluids, lower injection pressures (gas well at 1585 psi and water well at 1595 psi) make both criteria comparable for the novel foam (Table 6). This supports our preliminary conclusion drawn for the conventional foam above that the injection constraint is of much less importance and it is not necessary that the constant pressure will be beneficial. The foam performance is a function of injection rate or pressure, but the most determinative factor is surfactant properties.

4.2.3 CO₂ continuous injection with dissolved CO₂-soluble surfactant

The unique injection strategy, CO₂ continuous injection with dissolved novel surfactant, was examined. For sake of comparison, analogous to the manipulation in core flooding, CO₂ injection rate is the summary of two phases in alternating and co-injection strategies under surface conditions. Accordingly, the surfactant concentration is lowered to maintain the same amount of surfactant injected. Two perforation location scenarios are investigated as well as both injection constraints, as shown in Table 2.

4.2.3.1 Constant rate injection mode A significantly high CO₂ storage has been achieved, which is more than a 30% improvement over SINB, as shown in Table 7 and Fig. 39a. This is also implicitly indicated by the gas production rate that is far lower than the injection rate at time line (Fig. 40). It is observed that the gas “override zone” expands to the whole reservoir. The distinctions between full completion and partial completion through lower ten layers are reduced significantly indicated by the almost

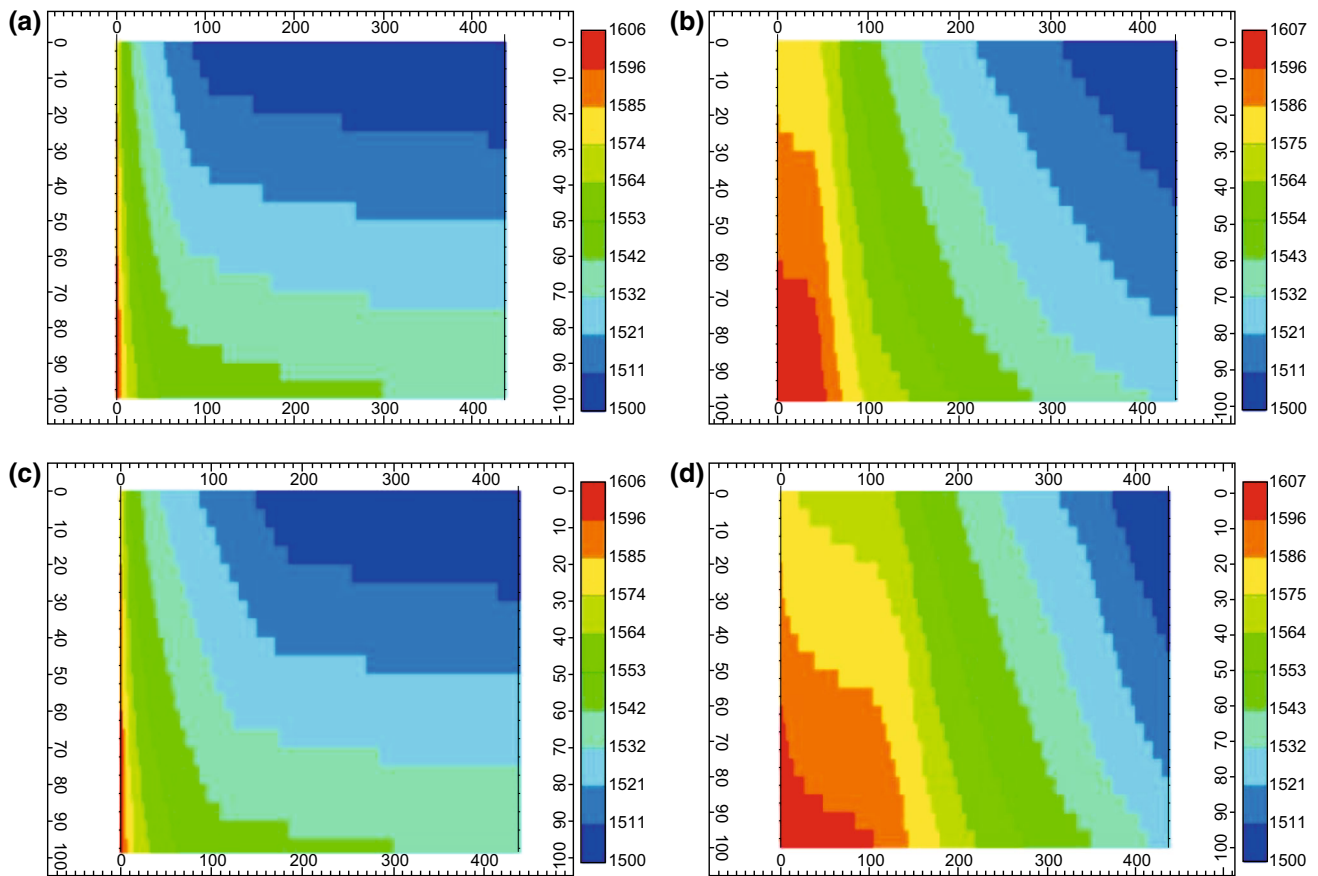


Fig. 30 Pressure distribution of small slug size (36.5 days) for **a** CD1045, **b** novel surfactant, and of larger slug size (182.5 days) for **c** CD1045, **d** novel surfactant during alternating injection under constant pressure constraint

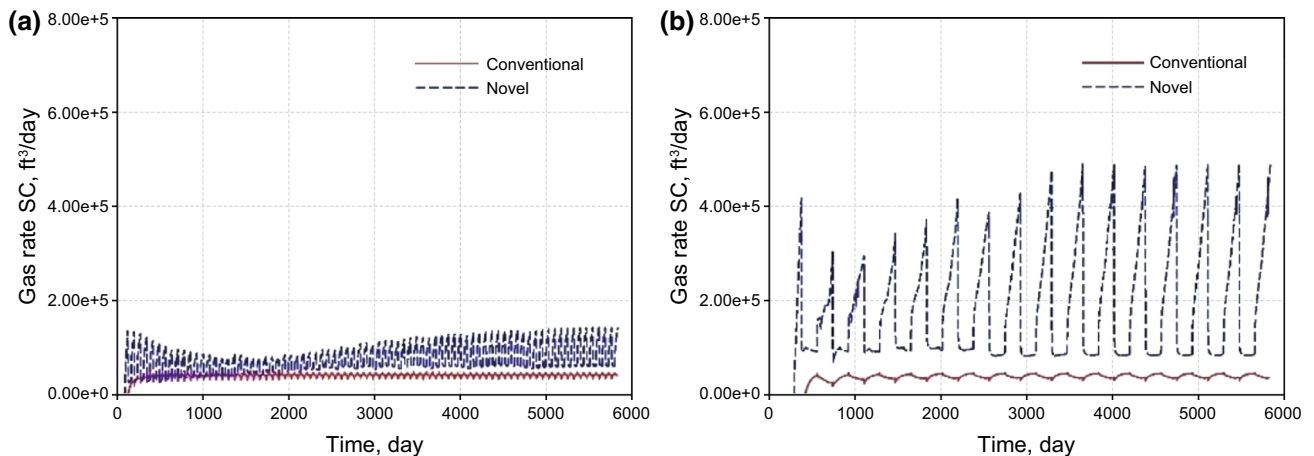


Fig. 31 Gas production rate of alternating injection under constant pressure constraint for **a** 36.5 days and **b** 182.5 days

identical gas production rate (Fig. 40), BHP in the injector (Fig. 41), gas saturation (not shown), surfactant concentration (not shown), and pressure distribution (not shown). Hence, we could take full completion for further discussion.

It may be biased to make the judgment now solely through CO₂ storage because we inject more CO₂. As shown in Table 7 and Fig. 39b, relative to SINB, this novel injection strategy improves the CO₂ utilization ratio by 3%. This can be perceived from the gas saturation profiles more

Table 6 Comparison of CO₂ storage and utilization ratio for constant rate and pressure injection modes for SINB

	CO ₂ storage, 10 ⁷ scf			CO ₂ utilization ratio		
	Constant rate	Constant pressure		Constant rate	Constant pressure	
		Gas (1608 psi) Water (1598 psi)	Gas (1585 psi) Water (1595 psi)		Gas (1608 psi) Water (1598 psi)	Gas (1585 psi) Water (1595 psi)
Novel	8.9	12.3	8.38	0.338	0.142	0.33
Conventional	1.73	1.44	–	0.066	0.0554	–

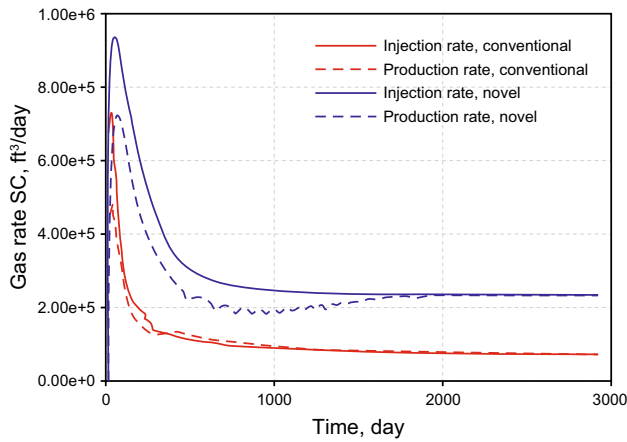


Fig. 32 Gas injection and production rates of novel and conventional foams for SINB with constant pressure constraint

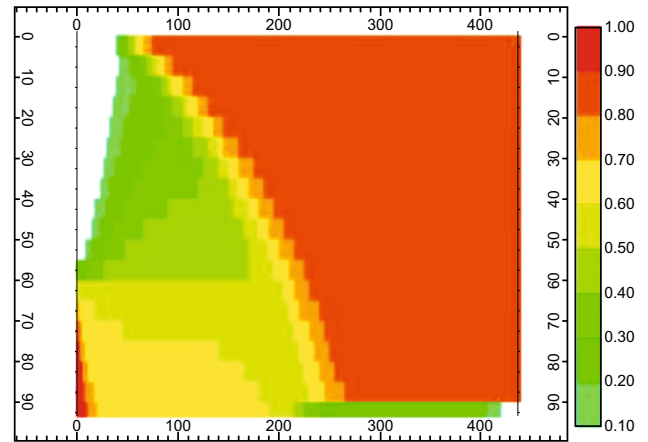


Fig. 34 Gas saturation of novel foam for SINB with constant pressure constraint

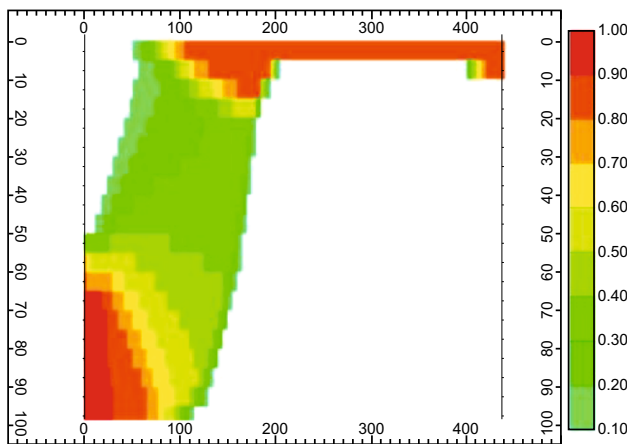


Fig. 33 Gas saturation of conventional foam for SINB with constant pressure constraint

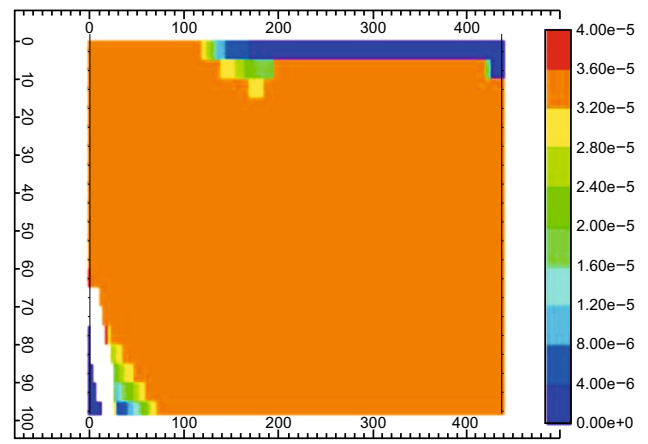


Fig. 35 Surfactant concentration of conventional foam for SINB with constant pressure constraint

directly, as shown in Fig. 42, which clearly illustrates a much more uniform gas propagation front. Furthermore, it is hard to tell the traditionally defined mixed zone which is already occupied by the so-called override zone. Surfactant concentration profiles (Fig. 43) displace a clear piston-like front of surfactant propagation. Meanwhile, it is important to note that there is a low concentration zone near the

wellbore that expands with time, which facilitates the improvement in injectivity. The reason of this phenomenon is different from that in the alternating injection with slug size increasing for the novel foam (Fig. 12b, d), which results from continuous extraction of fresh CO₂. Here, CO₂ is already saturated with surfactant and the extracted substance becomes water because the solubility of water in

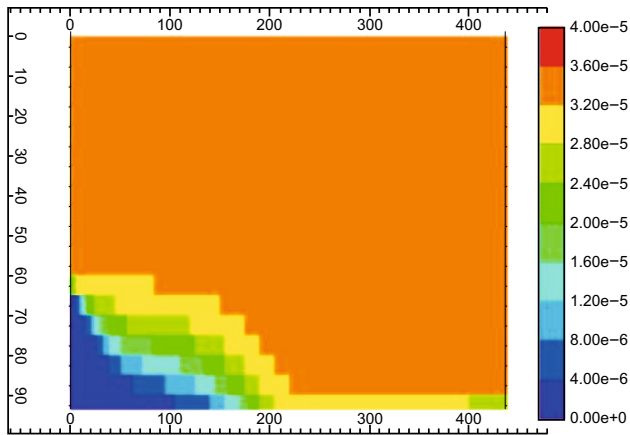


Fig. 36 Surfactant concentration of novel foam for SINB with constant pressure constraint

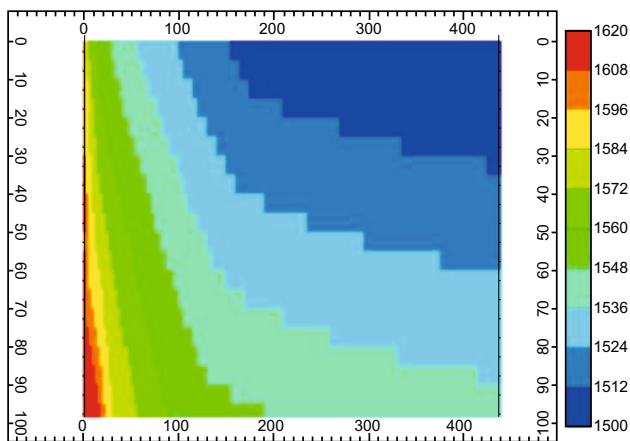


Fig. 37 Pressure distribution of conventional foam for SINB with constant pressure constraint

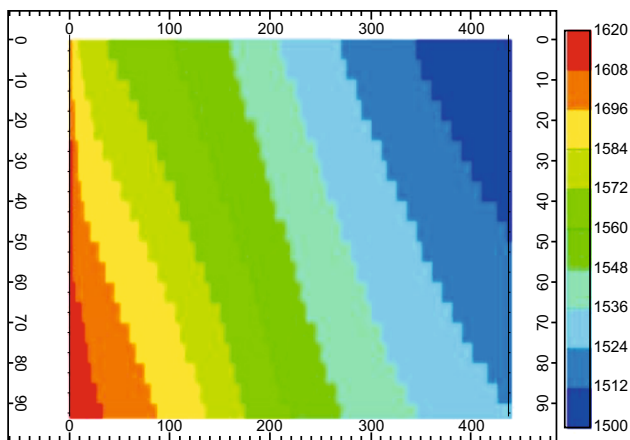


Fig. 38 Pressure distribution of novel foam for SINB with constant pressure constraint

CO₂ is not zero. With a huge amount of gas flow, bubbles will collapse when the water saturation approaches the critical value.

Here, without interference from water, the novel surfactant can be delivered much deeper into the reservoir and foam is generated in situ with formation water. It is straightforward to deduce that the injection pressure would be compellingly low among all the studied cases, as shown in Fig. 41, in which the partial completion gives a little higher value. The superiority of this novel strategy is also evidenced by the pressure distribution in the reservoir (Fig. 44). A high pressure gradient extends into the reservoir deeply, characterized by the extremely evenly distributed zones and steep contour lines, which stand for the high power utilization efficiency. In summary, this novel injection strategy is almost incomparably better with respect to saved water injection cost and highly improved sweep efficiency and gas utilization.

4.2.3.2 Constant pressure injection mode Now, we examine our conclusions for this novel injection strategy with full completion under a constant pressure injection constraint. Following the manipulations above, at first, we set an equivalent gas well injection pressure, 1585 psi, to chase the same amount of gas injection with that under the constant rate mode; then, a higher injection pressure is applied, 1610 psi, to validate our conclusions, as summarized in Table 8. It is likely that close CO₂ storage and utilization ratio are achieved with injection fluid conservation, while higher CO₂ storage and lower gas utilization efficiency occur with higher injection pressure. Again, this novel injection strategy greatly outperforms all other cases with respect to both criteria since more surfactants can be transported to the upper layers without interference of the water phase. It is noted that relative to the gradually declining injection rate in SINB (Fig. 32), the injection rate here (Fig. 45) showed the opposite trend. Meanwhile, the constant pressure constraint just improves the novel foam performance indicated by the almost identical gas saturation profiles (Figs. 46, 42), surfactant concentration profiles (Figs. 47, 43), and pressure distributions (Figs. 48, 44).

The performance of novel foam here (Table 8) supports our previous preliminary conclusions (Ren et al. 2013) that the novel foam performance is a function of injection strategy, injection rate or pressure, and partition coefficient. For certain injection strategies and novel surfactant, regardless of injection constraint, the sweep efficiency is a monotonic function of injection rate or pressure, but the gas utilization ratio demonstrates a parabolic shape. These

Table 7 Comparison of CO₂ storage and utilization ratio among different injection strategies with constant rate injection mode

	CO ₂ storage, 10 ⁷ scf			CO ₂ utilization ratio		
	Alternating injection (36.5-day slug size)	SINB	CO ₂ continuous injection with CO ₂ -soluble surfactant	Alternating injection (36.5-day slug size)	SINB	CO ₂ continuous injection with CO ₂ -soluble surfactant
Novel	7.36	8.9	11.7	0.28	0.338	0.348
Conventional	1.16	1.73	–	0.044	0.066	–

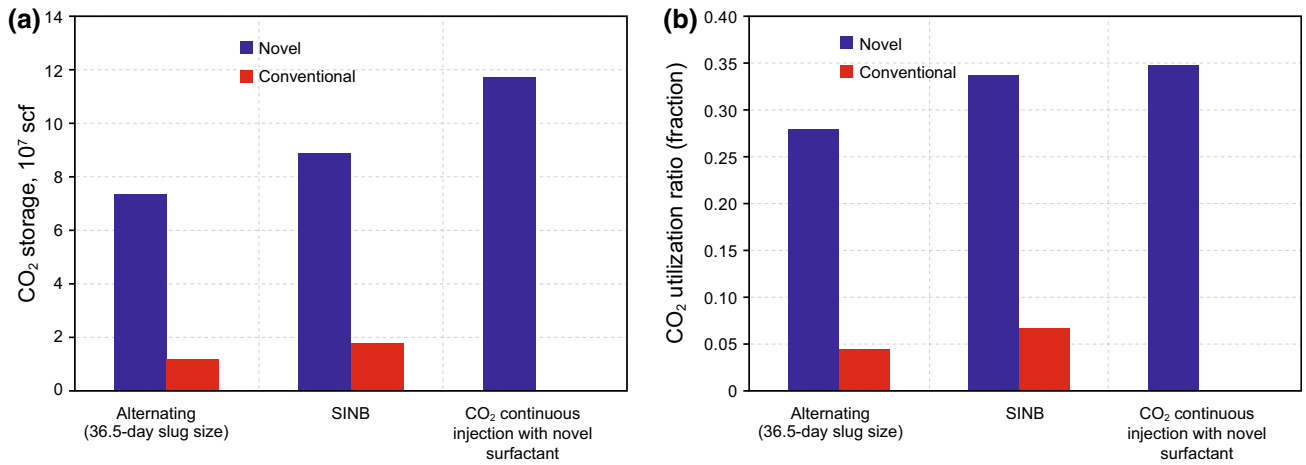


Fig. 39 Comparison of foam performances among different injection strategies. **a** CO₂ storage. **b** CO₂ utilization ratio

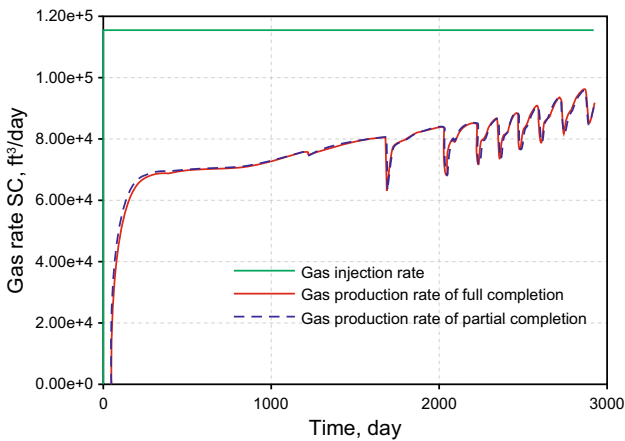


Fig. 40 Gas injection and production rates of CO₂ continuous injection with dissolved CO₂-soluble surfactant with full completion and partial completion

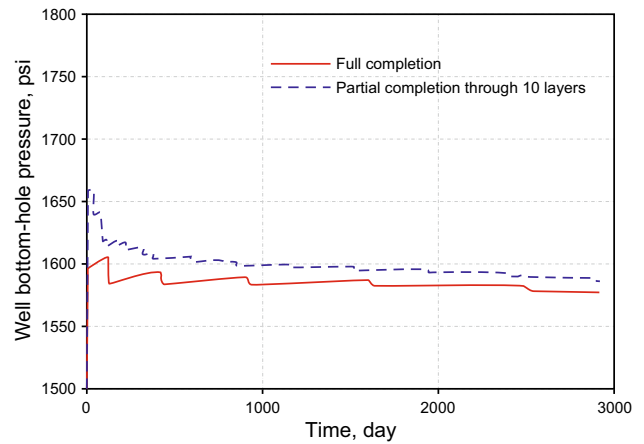


Fig. 41 Bottom-hole pressure in the gas injector of CO₂ continuous injection with dissolved CO₂-soluble surfactant with full completion and partial completion

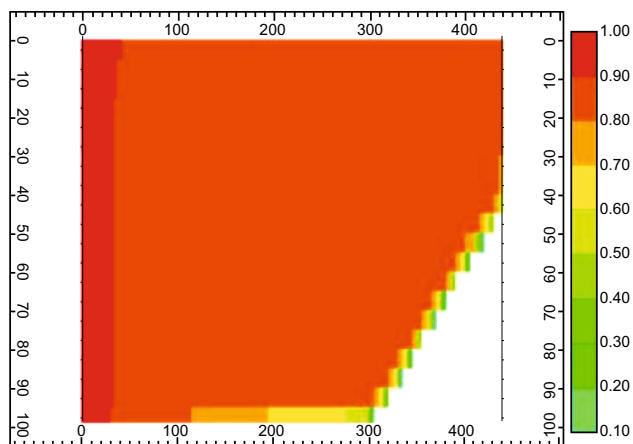


Fig. 42 Gas saturation of CO₂ continuous injection with dissolved CO₂-soluble surfactant with full completion

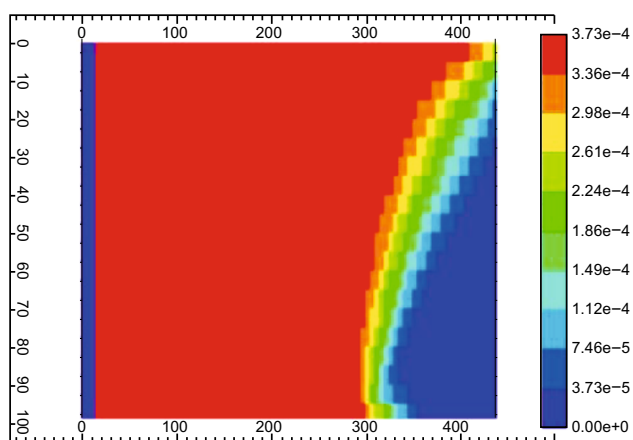


Fig. 43 Surfactant concentration of CO₂ continuous injection with dissolved CO₂-soluble surfactant with full completion

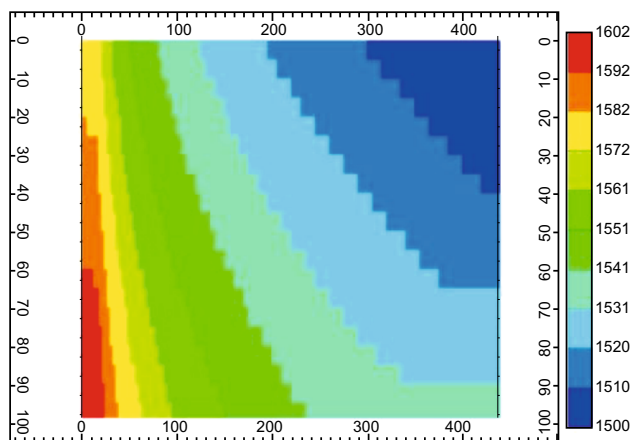


Fig. 44 Pressure distribution of CO₂ continuous injection with dissolved CO₂-soluble surfactant with full completion

conclusions highly improve the robustness of foam application according to field fluid requirement and facility availability.

5 Summary

In summary, the inherently superior properties of the novel surfactant make it outperform conventional surfactant in every injection strategy. The restriction of constant rate injection mode does not exist anymore. Injection constraint cannot solve the intrinsic problem that causes gas channeling because the constant pressure mode still arranges the pressure distribution through adjusting the injection rate (Boeije and Rossen 2014). Previous researchers (Shi and Rossen 1996, 1998; Shan and Rossen 2004; Rossen et al. 2006; Rossen and Shen 2007) have demonstrated that for conventional foam, the override zone will not expand downwards greatly and the only possible change is that the mixed zone spreads to a producer with stronger foam or higher injection pressure, as shown in Fig. 49 (black dash vs red dot dash lines), which will deteriorate injectivity. The red dot dash line indicates the cross-point of three zones could only move horizontally and this is the reason the gravity segregation length has attracted so much attention. Now, relative to the conventional foam, this novel foam tends to weaken the foam near the wellbore and strengthen it on the top layers with migration of surfactants with gas. In other words, the conflict between sweep efficiency and injectivity encountered by the conventional foam (Namdar and Rossen 2013) has been reduced significantly by the novel foam. Continuously supplying enough surfactants to the top layer is crucial for gas diversion to increase the volume of the traditionally defined override and mixed zones (Fig. 49 in blue solid line). Hence, R_g is only a criterion for fighting gravity segregation but not a sufficient condition to evaluate an injection strategy. The volume of the override zone and gravity segregation height play an important role in determining the sweep efficiency, which requires not only even pressure distribution but also steep pressure contour lines. The novel foam can perform well even with short segregation length or early gas breakthrough because they do not reflect the successive stages of gas diversion. Intrinsic superiority of the novel surfactant replaces the injection mode to dominate the foam process and gives more freedom to injection arrangement according to CO₂ acquirement.

Table 8 Comparison of CO₂ storage and utilization ratio for constant rate and pressure injection modes for the novel CO₂ injection

	CO ₂ storage, 10 ⁷ scf			CO ₂ utilization ratio		
	Constant rate	Constant pressure		Constant rate	Constant pressure	
		Gas (1585 psi)	Gas (1610 psi)		Gas (1585 psi)	Gas (1610 psi)
Novel	11.7	11.9	13.8	0.348	0.351	0.298

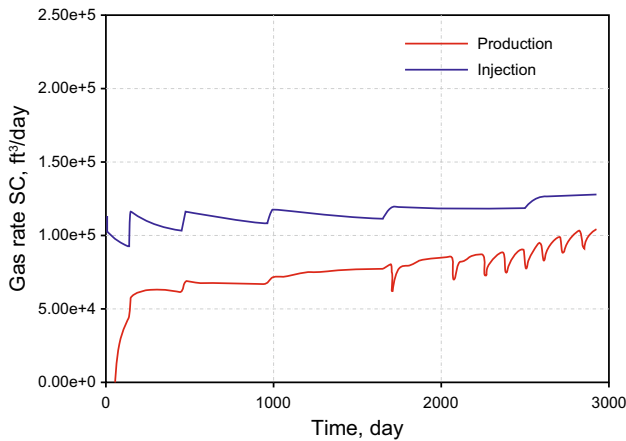


Fig. 45 Gas injection and production rates of CO₂ continuous injection with dissolved CO₂-soluble surfactant under constant pressure constraint (1585 psi)

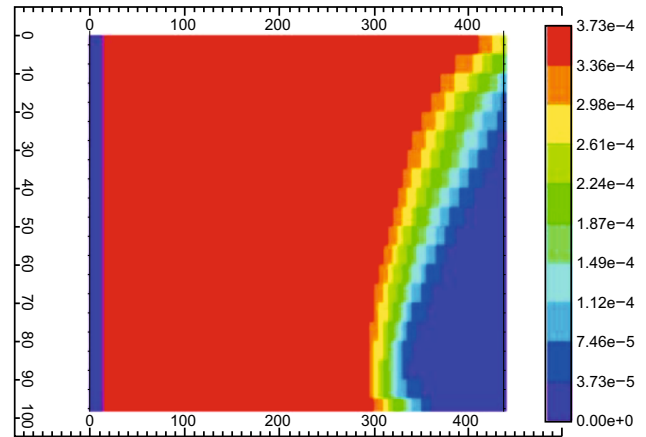


Fig. 47 Surfactant concentration of CO₂ continuous injection with dissolved CO₂-soluble surfactant under constant pressure constraint (1585 psi)

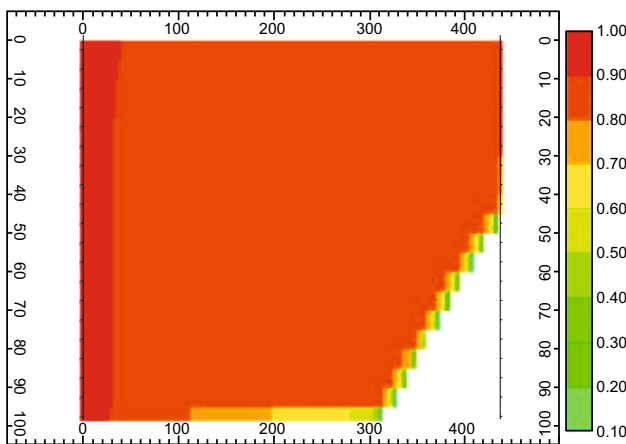


Fig. 46 Gas saturation of CO₂ continuous injection with dissolved CO₂-soluble surfactant under constant pressure constraint (1585 psi)

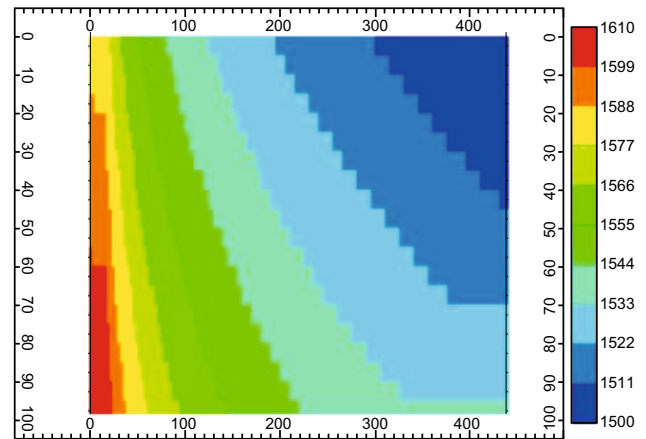


Fig. 48 Pressure distribution of CO₂ continuous injection with dissolved CO₂-soluble surfactant under constant pressure constraint (1585 psi)

6 Conclusions

(1) The novel CO₂-soluble surfactant provides better film stabilization ability than the conventional aqueous surfactant. In turn, when simultaneously injecting, the novel foam propagates faster and demonstrates higher pressure drop and sweep efficiency.

- (2) Alternating injection does improve the foam propagation and injectivity regardless of surfactant type. Alternating injection also promote the superiority of the novel foam over the conventional one in quicker and stronger foam generation.
- (3) It is the first time the novel injection strategy, CO₂ continuous injection with dissolved CO₂-soluble surfactant, has been tested in consolidated cores,

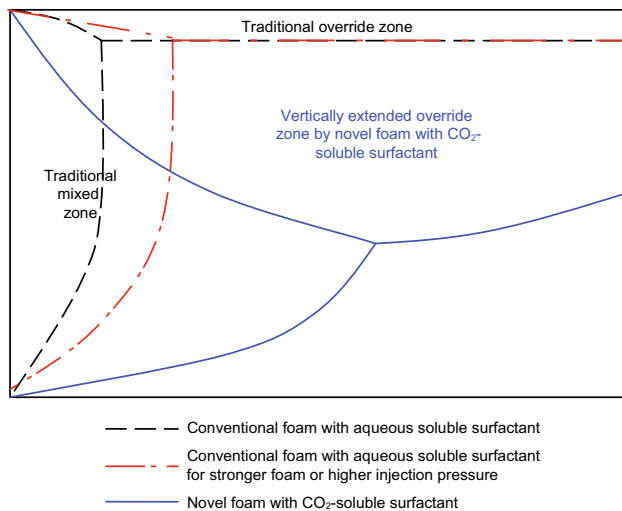


Fig. 49 Schematic plot of conventional and novel foams on fighting gravity segregation

which demonstrates superior surfactant transportation ability, in turn improving the foam propagation and displacement rate significantly.

- (4) With field scale simulation, for all tested injection strategies, regardless of constant rate or pressure constraint, the novel foam significantly outperforms conventional foam in terms of much higher sweep efficiency, injectivity and much more even pressure distribution resulting from intrinsic property of the novel surfactant.
- (5) The novel foam performance is a function of injection strategy, injection rate or pressure, and partition coefficient (not discussed here); for a fixed injection strategy and with the novel surfactant, regardless of injection constraint, sweep efficiency is a monotonic function of injection rate or pressure, but the gas utilization ratio demonstrates a parabolic shape.
- (6) Injection constraint, i.e., constant rate or pressure, is of much less importance to both types of foams, as long as similar amount of fluids have been injected. From the point view of sweep efficiency, for alternating injection, constant pressure mode tends to amplify the superiority of the novel foam over the conventional one due to higher injectivity.
- (7) Relative to conventional foam, the novel foam tends to increase the segregation height and volume of the traditionally defined override zone through gas diversion instead of solely increasing gravity segregation length and delaying gas breakthrough time. The latter two are of less importance in performance evaluation for the novel foam.
- (8) For alternating injection, relative to conventional foam that is preferential to larger slug, the novel

foam is not sensitive to injection fluid slug size regardless of injection constraint. The optimal slug size of novel foam with respect to gas utilization is a function of injection rate or pressure and partition coefficient.

- (9) Co-injection does lower the injectivity for conventional foam relative to alternating injection while this problem has been greatly reduced with the novel foam owing to surfactant concentration deduction by gas extraction.
- (10) For simultaneous injection through same sections (SIAP and SIPP), relative to full completion, partial completion lowers the injectivity and improves the sweep efficiency for both foams, while for separate injection (SINB and SIWB), the novel foam really reduces the distinction between them with respect to sweep efficiency and injectivity. The separate injection (SINB and SIWB) is able to give longer gravity segregation lengths and higher injectivity than simultaneous injection through same sections (SIAP and SIPP).
- (11) The novel injection strategy, continuous CO₂ injection with dissolved surfactant, gives the best foam performance among all the tested scenarios regardless of completion sections and injection constraint. This may dramatically lower the water injection/treatment cost and improve the robustness of foam application.

Acknowledgements The authors would like to thank Hang Zhang (University of Texas at Austin, currently at Schlumberger Houston) for his dedicated help with laboratory experiments.

Open Access This article is distributed under the terms of the Creative Commons Attribution 4.0 International License (<http://creativecommons.org/licenses/by/4.0/>), which permits unrestricted use, distribution, and reproduction in any medium, provided you give appropriate credit to the original author(s) and the source, provide a link to the Creative Commons license, and indicate if changes were made.

References

- Adkins SS, Chen X, Chan I, Torino E, Nguyen QP, Sanders AW, Johnston KP. Morphology and stability of CO₂-in-water foams with nonionic hydrocarbon surfactants. *Langmuir*. 2010a;26(8):5335–48. doi:10.1021/la903663v.
- Adkins SS, Chen X, Nguyen QP, Sanders AW, Johnston KP. Effect of branching on the interfacial properties of nonionic hydrocarbon surfactants at the air–water and carbon dioxide–water interfaces. *J Colloid Interface Sci*. 2010b;346(2):455–63. doi:10.1016/j.jcis.2009.12.059.
- Algharaib MK, Gharbi RB, Malallah A, Al-Ghanim W. Parametric investigations of a modified SWAG injection technique. In: SPE Middle East oil and gas show and conference, 11–14 March, Manama, Bahrain; 2007. doi:10.2118/105071-MS.

- Bernard G, Holm L. Method for recovering oil from subterranean formations. U.S. Patent. No.3342256. 19 Sep 1967.
- Blaker T, Celius HK, Lie T, Martinsen HA, Rasmussen L, Vassenden F. Foam for gas mobility control in the Snorre Field: the FAWAG project. In: SPE annual technical conference and exhibition, 3–6 October, Houston, Texas; 1999. doi:10.2118/56478-MS.
- Boeije CS, Rossen W. Gas-injection rate needed for SAG foam processes to overcome gravity override. SPE J. 2014;20(1):49–59. doi:10.2118/166244-PA.
- Bond DC, Holbrook CC. Gas drive oil recovery process. U.S. Patent. No. 2866507. Dec 1958.
- Chen X, Adkins SS, Nguyen QP, Sander AS, Johnston KP. Interfacial tension and the behavior of microemulsions and macroemulsions of water and carbon dioxide with a branched hydrocarbon nonionic surfactant. J Supercrit Fluids. 2010;55(2):712–23. doi:10.1016/j.supflu.2010.08.019.
- Chen Y, Elhag AS, Cui L, Worthen AJ, Reddy PP, Noguera JA, Ou AM, Ma K, Puerto M, Hirasaki GJ, Nguyen PQ, Biswal SL, Johnston KP. CO₂-in-water foam at elevated temperature and salinity stabilized with a nonionic surfactant with a high degree of ethoxylation. Ind Eng Chem Res. 2015;54(16):4252–63. doi:10.1021/ie503674m.
- Chen Y, Elhag AS, Poon BM, Cui L, Ma K, Liao SY, Johnston KP. Ethoxylated cationic surfactants for CO₂ EOR in high temperature, high salinity reservoirs. In: SPE annual technical conference and exhibition, 3–6 Oct, Houston, Texas; 2012. doi:10.2118/154222-MS.
- Cheng L, Reme AB, Shan D, Coombe DA, Rossen WR. Simulating foam processes at high and low foam qualities. In: SPE/DOE improved oil recovery symposium, 3–5 April, Tulsa, Oklahoma; 2000. doi:10.2118/59287-MS.
- Cui L, Ma K, Abdala AA, Lu J, Tanakov IM, Biswal SL, Hirasaki GJ. Adsorption of a switchable cationic surfactant on natural carbonate minerals. SPE J. 2014;20(1):70–8. doi:10.2118/169040-PA.
- Dhanuka V, Dickson J, Ryoo W, Johnston K. High internal phase CO₂-in-water emulsions stabilized with a branched nonionic hydrocarbon surfactant. J Colloid Interface Sci. 2006;298(1):406–18. doi:10.1016/j.jcis.2005.11.057.
- Du D, Zitha PLJ, Uijttenhout MGH. Carbon dioxide foam rheology in porous media: a CT scan study. SPE J. 2007;12(2):245–52. doi:10.2118/97552-PA.
- Eastoe J, Dupont A, Steytler DC, Thorpe M, Gurgel A, Heenan RK. Micellization of economically viable surfactants in CO₂. J Colloid Interface Sci. 2003;258(2):367–73. doi:10.1016/S0021-9797(02)00104-2.
- Eastoe J, Gold S, Steytler DC. Surfactants for CO₂. Langmuir. 2006;22(24):9832–42. doi:10.1021/la060764d.
- Eastoe J, Paul A, Nave S. Micellization of hydrocarbon surfactants in supercritical carbon dioxide. J Am Chem Soc. 2001;123:988–9. doi:10.1021/ja005795o.
- Elhag AS, Chen Y, Chen H, Reddy PP, Cui L, Worthen AJ, Johnston KP. Switchable amine surfactants for stable CO₂/brine foams in high temperature, high salinity reservoirs. In: SPE improved oil recovery symposium, 12–16 April, Tulsa, Oklahoma, USA; 2014. doi:10.2118/169041-MS.
- Fan X, Potluri VK, McLeod MC, Wang Y, Liu JC, Enick RM, Hamilton AD, Roberts CB, Johnson JK, Beckman EJ. Oxygenated hydrocarbon ionic surfactants exhibit CO₂ solubility. J Am Chem Soc. 2005;127(33):11754–62. doi:10.1021/ja052037v.
- Farajzadeh R, Lotfollahi M, Eftekhari AA, Rossen WR, Hirasaki GJ. Effect of permeability on implicit-texture foam model parameters and the limiting capillary pressure. Energy Fuels. 2015;29(5):3011–8. doi:10.1021/acs.energyfuels.5b00248.
- Fisher AW, Foulser RWS, Goodyear SG. Mathematical modeling of foam flooding. In: SPE/DOE enhanced oil recovery symposium, 22–25 April, Tulsa, Oklahoma; 1990. doi:10.2118/20195-MS.
- Friedmann F, Chen WH, Gauglitz PA. Experimental and simulation study of high-temperature foam displacement in porous media. SPE Reserv Eng. 1991;6(1):37–45. doi:10.2118/17357-PA.
- Grigg RB. Improving CO₂ efficiency for recovering oil in heterogeneous reservoirs. DOE Contract No. DE-FG26-01BC15364. 2004
- Hanssen JE, Surguchev LM, Svorstol I. SAG injection in a North Sea stratified reservoir: flow experiment and simulation. In: European petroleum conference, 25–27 Oct, London, United Kingdom; 1994. doi:10.2118/28847-MS.
- Heller JP. CO₂ foams in enhanced oil recovery. In: Schramm LL, editor. Foams: fundamentals and applications in the petroleum industry, vol. 242., ACS Advances in Chemistry Series Washington: American Chemical Society; 1994. p. 201. doi:10.1021/ba-1994-0242.ch005.
- Hoefling TA, Beitle RR, Enick RM, Beckman EJ. Design and synthesis of highly CO₂-soluble surfactants and chelating agents. Fluid Phase Equilib. 1993;83:203–12. doi:10.1016/0378-3812(93)87023-T.
- Hoefner ML, Evans EM, Buckles JJ, Jones TA. CO₂ foam: results from four developmental field trials. SPE Reserv Eng. 1995;10(4):273–81. doi:10.2118/27787-PA.
- Jamshidnezhad M, Shen C, Kool PH, Rossen WR. Well stimulation and gravity segregation in gas improved oil recovery. In: SPE international symposium and exhibition on formation damage control, 13–15 Feb, Lafayette, Louisiana, USA; 2008a. doi:10.2118/112375-MS.
- Jamshidnezhad M, van Der Bol L, Rossen WR. Injection of water above gas for improved sweep in gas IOR: performance in 3D. In: International petroleum technology conference, 3–5 Dec, Kuala Lumpur, Malaysia; 2008b. doi:10.2523/IPTC-12556-MS.
- Jenkins MK. An analytical model for water/gas miscible displacements. In: SPE enhanced oil recovery symposium, 15–18 April, Tulsa, Oklahoma; 1984. doi:10.2118/12632-MS.
- Kloet M, Renkema WJ, Rossen WR. Optimal design criteria for SAG foam processes in heterogeneous reservoirs. In: EUROPEC/EAGE conference and exhibition, 8–11 June, Amsterdam, The Netherlands; 2009. doi:10.2118/121581-MS.
- Lake LW. Enhanced oil recovery. New York: Prentice Hall; 1989.
- Lawson JB. The adsorption of non-ionic and anionic surfactants on sandstone and carbonate. In: SPE symposium on improved methods of oil recovery, 16–17 April, Tulsa, Oklahoma: Society of Petroleum Engineers; 1978. doi:10.2118/7052-MS.
- Lawson JB, Reisberg J. Alternate slugs of gas and dilute surfactant for mobility control during chemical flooding. In: SPE/DOE enhanced oil recovery symposium, 20–23 April, Tulsa, Oklahoma; 1980. doi:10.2118/8839-MS.
- Le VQ, Nguyen QP, Sanders A. A novel foam concept with CO₂ dissolved surfactants. In: SPE symposium on improved oil recovery, 20–23 April, Tulsa, Oklahoma, USA; 2008. doi:10.2118/113370-MS.
- Lee HO, Heller JP. Carbon dioxide foam mobility measurement at high pressure. In: Annual colloid and surface science symposium, 21–24 June, Ann Arbor, Michigan; 1988. ACS Symposium Series 373: 375–386.
- Leeftink TN, Latooij CA, Rossen WR. Injectivity errors in simulation of foam EOR. In: The 17th European symposium on improved oil recovery, St. Petersburg, Russia. 16–18 April 2013.
- Li B, Hirasaki GJ, Miller CA. Upscaling of foam mobility control to three dimensions. In: SPE/DOE symposium on improved oil recovery, 22–26 April, Tulsa, Oklahoma, USA; 2006. doi:10.2118/99719-MS.

- Li Q, Rossen WR. Injection strategies for foam generation in homogeneous and layered porous media. In: SPE annual technical conference and exhibition, 9–12 Oct, Dallas, Texas; 2005. doi:[10.2118/96116-MS](https://doi.org/10.2118/96116-MS).
- Liu J, Han B, Li G, Zhang X. Investigation of nonionic surfactant dynol-604 based reverse microemulsions formed in supercritical carbon dioxide. *Langmuir*. 2001;17(26):8040–3. doi:[10.1021/la010743d](https://doi.org/10.1021/la010743d).
- Liu M, Andrianov A, Rossen WR. Sweep efficiency in CO₂ foam simulations with oil. In: SPE EUROPEC/EAGE annual conference and exhibition, 23–26 May, Vienna, Austria; 2011. doi:[10.2118/142999-MS](https://doi.org/10.2118/142999-MS).
- Liu ZT, Erkey C. Water in carbon dioxide microemulsions with fluorinated analogues of AOT. *Langmuir*. 2001;17:274–7. doi:[10.1021/la000947e](https://doi.org/10.1021/la000947e).
- Ma K, Farajzadeh R, Lopez-Salinas JL, et al. Non-uniqueness, numerical artifacts, and parameter sensitivity in simulating steady-state and transient foam flow through porous media. *Transp Porous Media*. 2014;102:325. doi:[10.1007/s11242-014-0276-9](https://doi.org/10.1007/s11242-014-0276-9).
- Ma K, Lopez-Salinas JL, Puerto MC, Miller CA, Biswal SL, Hirasaki GJ. Estimation of parameters for the simulation of foam flow through porous media. Part 1: the dry-out effect. *Energy Fuels*. 2013;27(5):2363–75. doi:[10.1021/ef302036s](https://doi.org/10.1021/ef302036s).
- Ma TD, Youngren GK. Performance of immiscible water-alternating-gas (IWAG) injection at Kuparuk River Unit, North Slope, Alaska. In: SPE annual technical conference and exhibition, 25–28 September, New Orleans, Louisiana; 1994. doi:[10.2118/28602-MS](https://doi.org/10.2118/28602-MS).
- Mannhardt K, Schramm LL, Novosad JJ. Effect of rock type and brine composition on adsorption of two foam-forming surfactants. *SPE Adv Technol Ser*. 1993;1(1):212–8. doi:[10.2118/20463-PA](https://doi.org/10.2118/20463-PA).
- McHugh MA, Krukons VJ. *Supercritical fluid extraction*. 2nd ed. Boston: Butterworth; 1994.
- McLendon WJ, Koronaios P, Enick RM, Biesmans G, Salazar L, Miller A, Soong Y, McLendon T, Romanov V, Crandall D. Assessment of CO₂-soluble non-ionic surfactants for mobility reduction using mobility measurements and CT imaging. *J Pet Sci Eng*. 2014;119:196–209. doi:[10.1016/j.petrol.2014.05.010](https://doi.org/10.1016/j.petrol.2014.05.010).
- Mohd Shafian SR, Kamarul Bahrim R, Foo Y, Abdul Manap A, Tewari RD. Foam mobility control during WAG injection in a difficult reservoir with high temperature and high acid gas. In: SPE Asia Pacific enhanced oil recovery conference, 11–13 August, Kuala Lumpur, Malaysia; 2015. doi:[10.2118/174571-MS](https://doi.org/10.2118/174571-MS).
- Namdar Zanganeh M, Rossen W. Optimization of foam enhanced oil recovery: balancing sweep and injectivity. *SPE Res Eval Eng*. 2013;16(1):51–9. doi:[10.2118/163109-PA](https://doi.org/10.2118/163109-PA).
- O'Shea K, Kirmse K, Fox MA, Johnston KP. Polar and hydrogen-bonding interactions in supercritical fluids: effects on the tautomeric equilibrium of 4-(phenylazo)-1-naphthol. *J Phys Chem*. 1991;95:7863.
- Patzek TW. Field application of foam for mobility improvement and profile control. *SPE Reserv Eng*. 1996;11(2):79–85. doi:[10.2118/29612-PA](https://doi.org/10.2118/29612-PA).
- Ren G, Sanders AW, Nguyen QP. New method for the determination of surfactant solubility and partitioning between CO₂ and brine. *J Supercrit Fluids*. 2014;91:77–83. doi:[10.1016/j.supflu.2014.04.010](https://doi.org/10.1016/j.supflu.2014.04.010).
- Ren G, Zhang H, Nguyen Q. Effect of surfactant partitioning on mobility control during carbon-dioxide flooding. *SPE J*. 2013;18(4):752–65. doi:[10.2118/145102-PA](https://doi.org/10.2118/145102-PA).
- Rossen WR. Foams in enhanced oil recovery. In: Prud'homme RK, Khan SA, editors. *Foams: theory, measurements and applications*. New York: Marcel Dekker; 1995. p. 413–64.
- Rossen W, Boeije CS. Fitting foam-simulation-model parameters to data: II. surfactant-alternating-gas foam applications. *SPE Reserv Eval Eng*. 2015;18(2):273–83. doi:[10.2118/165282-PA](https://doi.org/10.2118/165282-PA).
- Rossen WR, Renkema WJ. Success of foam SAG processes in heterogeneous reservoirs. In: SPE annual technical conference and exhibition, 11–14 Nov, Anaheim, California, USA; 2007. doi:[10.2118/110408-MS](https://doi.org/10.2118/110408-MS).
- Rossen WR, Shen C. Gravity segregation in gas-injection IOR. In: EUROPEC/EAGE conference and exhibition, 11–14 June, London, UK; 2007. doi:[10.2118/107262-MS](https://doi.org/10.2118/107262-MS).
- Rossen WR, van Duijn CJ. Gravity segregation in steady-state horizontal flow in homogenous reservoirs. *J Pet Sci Eng*. 2004;43(1–2):99–111. doi:[10.1016/j.petrol.2004.01.004](https://doi.org/10.1016/j.petrol.2004.01.004).
- Rossen WR, Kibodeaux KR, Shi JX, Zeilinger SC, Lim MT. Injectivity and gravity override in surfactant-alternating-gas foam processes. In: SPE annual technical conference and exhibition, 22–25 Oct, Dallas, Texas; 1995a. doi:[10.2118/30753-MS](https://doi.org/10.2118/30753-MS).
- Rossen WR, van Duijn CJ, Nguyen QP, Vikingstad AK. Injection strategies to overcome gravity segregation in simultaneous gas and liquid injection in homogeneous reservoirs. In: SPE/DOE symposium on improved oil recovery, 22–26 April, Tulsa, Oklahoma, USA; 2006. doi:[10.2118/99794-MS](https://doi.org/10.2118/99794-MS).
- Rossen WR, Zeilinger SC, Shi J, Lim MT. Mechanistic simulation of foam processes in porous media. In: SPE annual technical conference and exhibition, 25–28 Sep, New Orleans, Louisiana; 1994. doi:[10.2118/28940-MS](https://doi.org/10.2118/28940-MS).
- Rossen WR, Zhou ZH, Mamun CK. Modeling foam mobility in porous media. *SPE Adv Technol Ser*. 1995b;3(1):146–53. doi:[10.2118/22627-PA](https://doi.org/10.2118/22627-PA).
- Sagir M, Tan IM, Mushtaq M, Ismail L, Nadeem M, Azam MR. Synthesis of a new CO₂ philic surfactant for enhanced oil recovery applications. *J Dispers Sci Technol*. 2014a;35(5):647–54. doi:[10.1080/01932691.2013.803253](https://doi.org/10.1080/01932691.2013.803253).
- Sagir M, Tan IM, Mushtaq M, et al. Novel surfactant for the reduction of CO₂/brine interfacial tension. *J Dispers Sci Technol*. 2014b;35(3):463–70. doi:[10.1080/01932691.2013.794111](https://doi.org/10.1080/01932691.2013.794111).
- Sagir M, Tan IM, Mushtaq M, Nadeem M. CO₂ mobility and CO₂/brine interfacial tension reduction by using a new surfactant for EOR applications. *J Dispers Sci Technol*. 2014c;35(11):1512. doi:[10.1080/01932691.2013.859087](https://doi.org/10.1080/01932691.2013.859087).
- Sagir M, Tan IM, Mushtaq M, Talebian SH. FAWAG using CO₂-philic surfactants for CO₂ mobility control for enhanced oil recovery applications. In: SPE Saudi Arabia section technical symposium and exhibition, 21–24 April, Al-Khobar, Saudi Arabia; 2014d. doi:[10.2118/172189-MS](https://doi.org/10.2118/172189-MS).
- Sanchez NL. Management of water alternating gas (WAG) injection projects. In: Latin American and Caribbean petroleum engineering conference, 21–23 April, Caracas, Venezuela; 1999. doi:[10.2118/53714-MS](https://doi.org/10.2118/53714-MS).
- Sanders A, Jones RM, Rabie A, Putra E, Linroth MA, Nguyen QP. Implementation of a CO₂ foam pilot study in the SACROC Field: performance evaluation. In: SPE annual technical conference and exhibition, 8–10 Oct, San Antonio, Texas, USA; 2012. doi:[10.2118/160016-MS](https://doi.org/10.2118/160016-MS).
- Sanders A, Nguyen QP, Nguyen N, Adkins S, Johnston KP. Twin-tailed surfactants for creating CO₂-in-water macroemulsions for sweep enhancement in CO₂-EOR. In: Abu Dhabi international petroleum exhibition and conference, 1–4 Nov, Abu Dhabi, UAE; 2010. doi:[10.2118/137689-MS](https://doi.org/10.2118/137689-MS).
- Shan D, Rossen WR. Optimal injection strategies for foam IOR. *SPE J*. 2004;9(2):132–50. doi:[10.2118/88811-PA](https://doi.org/10.2118/88811-PA).
- Shi JX, Rossen WR. Simulation and dimensional analysis of foam processes in porous media. In: Permian Basin oil and gas recovery conference, 27–29 March, Midland, Texas; 1996. doi:[10.2118/35166-MS](https://doi.org/10.2118/35166-MS).

- Shi JX, Rossen WR. Improved surfactant-alternating-gas foam process to control gravity override. In: SPE/DOE improved oil recovery symposium, 19–22 April, Tulsa, Oklahoma; 1998. doi:[10.2118/39653-MS](https://doi.org/10.2118/39653-MS).
- Stalkup FI Jr. Miscible displacement. SPE Monograph No. 8. New York: Society of Petroleum Engineers of AIME; 1983.
- Soong Y, Xing D, Wei B, Enick R M, Eastoe J, et al. CO₂-soluble surfactants for enhanced oil recovery mobility control via thickening or in-situ foam generation. In: Proc., 2009 AIChE Annual Meeting, Nashville, TN, USA; 8–13 Nov 2009.
- Stevens JE. CO₂ foam field verification pilot test at EVGSAU: phase IIIB–project operations and performance review. SPE Reserv Eng. 1995;10(4):266–72. doi:[10.2118/27786-PA](https://doi.org/10.2118/27786-PA).
- Stone HL. A simultaneous water and gas flood design with extraordinary vertical gas sweep. In: SPE international petroleum conference in Mexico, 7–9 Nov, Puebla Pue., Mexico; 2004a. doi:[10.2118/91724-MS](https://doi.org/10.2118/91724-MS).
- Stone HL. Method for improved vertical sweep of oil reservoirs. US Patent No. 7303006 (PCT/US2004/014519). 2004b.
- Stone HL. Vertical, conformance in an alternating water-miscible gas flood. In: SPE annual technical conference and exhibition, 26–29 Sep, New Orleans, Louisiana; 1982. doi:[10.2118/11130-MS](https://doi.org/10.2118/11130-MS).
- Svorstol I, Vassenden F, Mannhardt K. Laboratory studies for design of a foam pilot in the Snorre Field. In: SPE/DOE improved oil recovery symposium, 21–24 April, Tulsa, Oklahoma; 1996. doi:[10.2118/35400-MS](https://doi.org/10.2118/35400-MS).
- Tan B, Cooper AI. Functional oligo(vinyl acetate) CO₂-philes for solubilization and emulsification. J Am Chem Soc. 2005;127(25):8938–9. doi:[10.1021/ja052508d](https://doi.org/10.1021/ja052508d).
- Xing D, Wei B, McLendon WJ, Enick RM, McNulty S, Trickett K, Soong Y. CO₂-soluble, nonionic, water-soluble surfactants that stabilize CO₂-in-brine foams. SPE J. 2012;17(4):1172–85. doi:[10.2118/129907-PA](https://doi.org/10.2118/129907-PA).
- Xu Q, Rossen WR. Experimental study of gas injection in surfactant-alternating-gas foam process. In: SPE annual technical conference and exhibition, 5–8 Oct, Denver, Colorado; 2003. doi:[10.2118/84183-MS](https://doi.org/10.2118/84183-MS).
- Zeng YC, Ma K, Farajzadeh R, Puerto M, Biswal SL, Hirasaki GJ. Effect of surfactant partitioning between gaseous phase and aqueous phase on CO₂ foam transport for enhanced oil recovery. Transp Porous Media. 2016;114:777–93. doi:[10.1007/s11242-016-0743-6](https://doi.org/10.1007/s11242-016-0743-6).